Low-Energy K-N Scattering and $SU(3)$ Invariance*

ROBERT L. WARNOCK
Illinois Institute of Technology, Chicago, Illinois
and
Argonne National Laboratory, Argonne, Illinois

AND

GRAHAM FRYE
City College of the City University of New York, New York, New York
(Received 14 January 1965)

Phase shifts from K_+-p and K_+-d scattering up to 800 MeV/c are fitted by a sum of single-particle exchange terms and a "background" term representing unknown short-range forces. The background is described by a low-order polynomial in s and t in the invariant amplitudes. The single-particle states in the u-channel are Λ, Σ, Y_1^*(1385 MeV), Y_0^*(1405 MeV), Y_1^*(1520 MeV), and Y_1^*(1660 MeV). A continuum of u-channel $\bar{K}$-N scattering below 400 MeV/c is also included. In the t channel the states are ρ and a fictitious particle χ which is supposed to represent the average effect of ω and φ. The $Y^*N\bar{K}$ coupling constants are known from experiment or a combination of theory and experiment. The ratio of vector to tensor ρNN coupling constants is taken from nucleon electromagnetic-structure data. The other coupling constants are regarded as free parameters to be determined by fitting K-N data. For good fits it is necessary to retain the first three orders in the expansion of the background term. This entails eight free parameters. Two sets of fits to the data are found, one with the Fermi-type $I=0$ phase shifts ($\delta_{p3/2}$ large and positive) and one with Yang-type $I=0$ phases ($\delta_{p1/2}$ large and positive). In the Fermi case the Σ and ρ coupling constants each differ by more than five standard deviations from predictions based on $SU(3)$ symmetry. The Σ constant also disagrees badly with results from forward-angle dispersion relations. In the case of the Yang-type phase shifts, the coupling constants are essentially in agreement with $SU(3)$ predictions. In the Yang case the ρ term is necessary for an acceptable fit, in spite of the large number of parameters. The parameters for χ exchange are badly determined by the data, so there is no possibility of working with ω and φ coupling constants as separate free parameters. Exchange of scalar particles is considered as a model for the effects of "ABC" or "σ" π-π interactions at 310 or 400 MeV, and the K_1-K_1 interaction at 1000 MeV. Inclusion of such exchange terms affects the parameter values of the other terms only slightly, and therefore does not change the qualitative character of the fits to the data. The Y^* terms can also be omitted without changing the general character of the fits. They are not small, but they are well represented by the background terms. Unitarity corrections are estimated to be rather minor; they do not change the main conclusions.

I. THEORY BASED ON THE CINI-FUBINI REPRESENTATION OF THE SCATTERING AMPLITUDE

ACCORDING to the ideas of Mandelstam,[1] a theory of K-N scattering must simultaneously take into account the three processes that are related by the crossing principle; viz., $K+N\to K+N$, $\bar{K}+N\to\bar{K}+N$, and $K+\bar{K}\to N+\bar{N}$. We describe a systematic but partly phenomenological theory based on this viewpoint. Some important parts of the scattering amplitude are illustrated in Fig. 1. X is any particle, resonance, or two-body scattering state with the quantum numbers of the u channel ($\bar{K}+N\to\bar{K}+N$). ξ has the quantum numbers of the t channel ($K+\bar{K}\to N+\bar{N}$). Some of the coupling constants of the vertices pictured are known from measurements or from a combination of theory and measurements. The others we attempt to determine by a comparison of our theory with experiment. Besides the simplest terms of Fig. 1, one has the contributions of complicated many-particle states in the u and t channels and the effects of unitarity which may be visualized as "rescattering" in the s channel ($K+N\to K+N$). States X and ξ of low mass produce the singularities lying closest to the low-energy physical region. The background produced by states of higher mass (equivalently, by short-range forces) is not expected to be small, but at least one can hope that in the experimental region it will be a slowly varying function of the invariants $s=(p_1+q_1)^2$ and $t=(q_1-q_2)^2$, where p_i and q_i are the four-momenta of the particles as shown in Fig. 1. Following Cini and Fubini,[2] we represent this background by low-order polynomials in s and t in the invariant amplitudes. Specifically, let the scattering

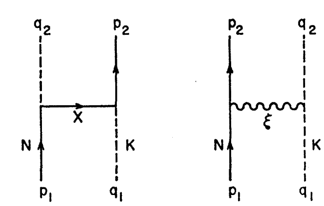

FIG. 1. Feynman graphs showing u-channel states X and t-channel state ξ.

* Work done partly under the auspices of the U. S. Atomic Energy Commission.

[1] S. Mandelstam, Phys. Rev. **115**, 1741 (1959).

[2] M. Cini and S. Fubini, Ann. Phys. (N. Y.) **3**, 352 (1960); see also J. Bowcock, W. M. Cottingham, and D. Lurié, Nuovo Cimento **16**, 918 (1960).

TABLE I. The states X and ξ of Fig. 1.

u-channel states X			t-channel states ξ		
X	Mass (MeV)	J^P	ξ	Mass (MeV)	J^{PG}
Λ	1115	$\frac{1}{2}^+$	ρ	750	1^{-+}
Σ	1190	$\frac{1}{2}^+$	ω	780	1^{--}
Y_1^*	1385	$\frac{3}{2}^+$	φ	1020	1^{--}
Y_0^*	1405	$\frac{1}{2}^-?$			
Y_0^*	1520	$\frac{3}{2}^-$			
Y_1^*	1660	$\frac{3}{2}^-?$			

amplitude for isospin I be given as[3]

$$T^{(I)}=\bar{u}(p_2,q_2)\times\left[-A^{(I)}(s,t)+\frac{i}{2}\gamma\cdot(q_1+q_2)B^{(I)}(s,t)\right]u(p_1,q_1)\,,\quad(1.1)$$

where u is a Dirac spinor, $\gamma=[\gamma_\mu]$ is a four-vector of Dirac matrices, and $A^{(I)}$ and $B^{(I)}$ are the invariant amplitudes. Then the distant singularities are represented by "remainder" functions A_r, B_r as follows:

$$\begin{aligned}A_r^{(I)}&=\alpha^{(I)}+\alpha_s^{(I)}s+\alpha_t^{(I)}t+\cdots\\B_r^{(I)}&=\beta^{(I)}+\cdots.\end{aligned}\quad(1.2)$$

The terms in α, β, and $\alpha_{s,t}$ represent the zeroth, first, and second orders of approximation, respectively, if orders are assigned by dimensions of the constants.

The resonances listed in Table I are all included as zero-width "particles."[4] With more effort one could account for widths, but such a refinement might not be worthwhile at the present stage of the theory. Besides the states of Table I, we also make some attempt to account for the "ABC" phenomenon,[4] which has been interpreted as a strong s-wave π-π interaction peaking at about 310 MeV. We represent it by exchange of a $J^P=0^+$ particle with mass 310 MeV. This zero-width assumption may be questionable. However, we find that in fitting the data introduction of an $I=0$, 0^+ particle-exchange term always has a fairly small effect on the best-fit values of parameters, rather independently of the mass of the 0^+ particle. In fact, we have tried three different masses: 310 MeV for the ABC, 400 MeV for the 0^+ σ meson postulated by Brown and Singer,[5] and 1000 MeV for the apparent 0^+ K_1-K_1 interaction observed by Erwin *et al.*[6] In each case the data fits are only mildly perturbed by the 0^+ exchange. This circumstance leads us to think we need not worry much about $I=0$, 0^+ states in the t channel. In the present experimental situation this is fortunate for our analysis, since it may turn out that none of the three states mentioned actually exists as anything like a resonance. A recent search for the ABC in π-p collisions gave a negative result,[7] and the σ and K_1-K_1 interactions are based on somewhat limited evidence.

Some known resonances of higher mass and of uncertain spin and parity are not included explicitly. We assume that their effects can be represented by the remainder terms of Eq. (1.2), or that they couple weakly to our system, or that their quantum numbers are such that they cannot enter the problem at all. The firmly established resonances which are omitted are Y_0^*(1815 MeV),[4] f_0(1250 MeV),[4] B(1220 MeV),[8] X_0(960 MeV),[9] A_1(1090 MeV),[4] and A_2(1300 MeV).[10] Also, one group has reported a broad isoscalar ρ-π resonance at 975 MeV.[11] The Y_0^*(1815 MeV) couples strongly to $\bar{K}$-N, so perhaps its effects should be considered eventually. For the present we argue that its large mass should enable us to represent it by the remainder terms. This point of view is supported by our study of the other Y^* terms, which have considerably smaller mass (compare Secs. II and III). The f_0, B, and A_1 have not been observed to decay into K-$\bar{K}$, as far as we know, which gives us some reason for neglecting them. The A_1 may have $J^P=2^-$ or 1^+, in which case its coupling to K-$\bar{K}$ is forbidden by parity conservation. The A_2 is supposed to have $I=1$ and $J^{PG}=2^{+-}$, and its decay into K-$\bar{K}$ has been observed. Goldhaber *et al.*[12] have reported the branching ratios $\rho\pi:\eta\pi:K\bar{K}=3:1:1$. The A_2 has a relatively small K-$\bar{K}$ partial width and a relatively large mass, so we may be justified in representing A_2 exchange only by the background terms. The X_0 is thought to be a 0^{-+} state, in which case it does not enter our problem, because of parity conservation. If the 975-MeV ρ-π resonance turns out to have quantum numbers allowing it to enter our problem, it will complicate an already difficult situation concerning $I=0$ particles in the t channel. The difficulty is that K-N scattering data seem to be very ineffective in constraining parameters associated with such particles (cf. Sec. II). Fortunately,

[3] G. F. Chew, M. L. Goldberger, F. Low, and Y. Nambu, Phys. Rev. **106**, 1337 (1957).

[4] For references to the experimental data, see, for example, R. H. Dalitz, Ann. Rev. Nucl. Sci. **13**, 339 (1963); G. Puppi, *ibid.* **13**, 287 (1963); M. Roos, Nucl. Phys. **52**, 1 (1964); A. H. Rosenfeld, A. Barbaro-Galtieri, W. H. Barkas, P. L. Bastien, J. Kirz, and Matts Roos, Rev. Mod. Phys. **36**, 977 (1964).

[5] L. Brown and P. Singer, Phys. Rev. **133**, B812 (1964); S. H. Patil, Phys. Rev. Letters **13**, 261 (1964).

[6] A. R. Erwin, G. A. Hoyer, R. H. March, W. D. Walker, and T. P. Wangler, Phys. Rev. Letters **9**, 34 (1962); G. Alexander, O. I. Dahl, L. Jacobs, G. R. Kalbfleisch, D. H. Miller, A. Rittenberg, J. Schwartz, and G. A. Smith, *ibid.* **9**, 460 (1962).

[7] I. M. Blair *et al.*, Phys. Letters **11**, 79 (1964).

[8] M. Abolins, R. L. Lander, W. A. W. Mehlhop, N. h. Xuong, P. M. Yager, Phys. Rev. Letters **11**, 381 (1963); D. D. Carmony *et al.*, *ibid.* **12**, 254 (1964).

[9] G. R. Kalbfleisch *et al.*, Phys. Rev. Letters **12**, 527 (1964); M. Goldberg *et al.*, *ibid.* **12**, 546 (1964); P. M. Dauber *et al.*, *ibid.* **13**, 449 (1964).

[10] G. Goldhaber, J. L. Brown, S. Goldhaber, J. A. Kady, K. B. C. Shen, and G. H. Trilling Phys. Rev. Letters **12**, 336 (1964); S. U. Chung, O. I. Dahl, L. M. Hardy, R. I. Hess, G. R. Kalbfleisch, *ibid.* **12**, 621 (1964); M. Aderholz *et al.*, Phys. Letters **10**, 226 (1964); J. F. Allard *et al.*, *ibid.* **10**, 143 (1964). A. Bettini *et al.*, Padua preprint; J. Alitti, J. P. Baton, B. Deler, M. Neveu-Rene, J. Crussard, *et al.*, Phys. Letters **15**, 69 (1965).

[11] J. Bartsch *et al.*, Phys. Letters **11**, 167 (1964).

[12] G. Goldhaber *et al.*, in Proceedings of the International Conference on High Energy Nuclear Physics, Dubna, USSR, 1964 (to be published).

the Dalitz plots of Bartsch *et al.*[11] favor $J^P=1^+, 2^-$, etc., in which case the state does not enter our analysis.

Among the states listed in Table I, two have uncertain spin and parity; viz., $Y_0^*(1405 \text{ MeV})$ and $Y_1^*(1660 \text{ MeV})$. The Y_0^* is assumed to be the Dalitz-Tuan[13] "virtual $\bar{K}$-N bound state" with $J^P=\frac{1}{2}^-$. This picture is compatible with low-energy $\bar{K}$-N scattering data and also with the fact that strong attractive forces in the $\frac{1}{2}^-$ $\bar{K}$-N state result from vector meson exchange. An alternative picture of $Y_0^*(1405 \text{ MeV})$ was proposed by Schwinger on the basis of a $U(3)\times U(3)$ symmetry scheme.[14] In Schwinger's theory, Y_0^* has $J^P=\frac{1}{2}^+$. Our discussion effectively covers this possibility, for the following reason. The $\frac{1}{2}^-$ Y_0^* term, which we always include, turns out to be negligibly small. On the other hand, a $\frac{1}{2}^+ Y_0^*$ is practically indistinguishable in its effect on K-N scattering from the Λ term. The Λ-Y_0^* mass difference has little effect. Thus, with a reinterpretation of the number we call the ΛNK coupling constant, Schwinger's Y_0^* is accounted for. The $Y_1^*(1660 \text{ MeV})$ is taken to be a $\frac{3}{2}^-$ state. This assignment is based on the recent experiment of Connolly *et al.*[15] We find that our results are virtually identical if we take $J^P=\frac{3}{2}^+$.[16] The reason is that the large mass and small $\bar{K}$-N branching fraction of Y_1^* guarantee that its effect on K-N scattering is very small for either parity assignment.

Besides the sharp resonances and particles of Table I, we also investigate the effect of s-wave $\bar{K}$-N scattering in the u channel. We consider only the momentum interval between 0 and 400 MeV/c laboratory momentum, in which the scattering is parametrized by the Humphrey-Ross[17] complex scattering lengths. Humphrey and Ross have two possible sets of scattering lengths, but that ambiguity causes us no trouble. With either set an evaluation of the u-channel integral for $\bar{K}$-N s-wave scattering results in a number which is entirely negligible. The results are tabulated in Sec. III. Because of their smallness, these terms are omitted in the data fits.

The various particle-exchange terms may be calculated as the Born approximations of the following Lagrangian densities:

$$u \text{ channel}, J^P=\tfrac{1}{2}^{-,+}: \quad G\bar{\psi}(1,\gamma_5)\Psi\phi+\text{h.c.}, \tag{1.3a}$$

$$u \text{ channel}, J^P=\tfrac{3}{2}^{-,+}:$$
$$(H/m)\tfrac{1}{2}(\partial_\mu\bar{\psi}\phi-\bar{\psi}\partial_\mu\phi)(1,\gamma_5)\Psi^\mu+\text{h.c.}, \tag{1.3b}$$

$$t \text{ channel}, J^P=0^+: \quad g\bar{\psi}\psi\varphi+mh\phi^\dagger\phi\varphi, \tag{1.3c}$$

$$t \text{ channel}, J^P=1^-:$$
$$\gamma^{(1)}\bar{\psi}\gamma_\mu\psi\varphi^\mu+(\gamma^{(2)}/2m)\bar{\psi}\sigma_{\mu\nu}\psi(\partial^\mu\varphi^\nu-\partial^\nu\varphi^\mu) +i\gamma(\partial_\mu\phi^\dagger\phi-\phi^\dagger\partial_\mu\phi)\varphi^\mu. \tag{1.3d}$$

The nucleon and K-meson fields are represented by ψ and ϕ, respectively, while Ψ and Ψ^μ represent $J=\frac{1}{2}$ and $J=\frac{3}{2}$ (Rarita-Schwinger) hyperon fields. Scalar and vector boson fields are denoted by φ and φ^μ. The nucleon mass m is introduced to make coupling constants dimensionless. The interactions as given in Eq. (1.3) are for isospin zero for exchanged particles. For exchange of isospin one in the u channel one replaces $\bar{\psi}\phi$ by $\bar{\psi}\tau\phi$ in Eq. (1.3a) and Eq. (1.3b). For isospin one in the t channel one replaces $\bar{\psi}\psi$ and $\phi^\dagger\phi$ by $\bar{\psi}\boldsymbol{\tau}\psi$ and $\phi^\dagger\boldsymbol{\tau}\phi$ in Eq. (1.3d).[18] Formulas for the partial-wave projections of the single-particle exchange terms are to be found in the Appendix.

The single-particle exchange terms may also be calculated by introducing delta functions in the appropriate absorptive parts appearing in the dispersion relations. By comparing the pole residues obtained in this way to those found by the Lagrangian calculation, we may relate some of the coupling constants to measured resonance parameters. For instance, for a $J=\frac{3}{2}$ state in the u channel we have

$$\frac{H^2}{4\pi}=\frac{3(Mm)^2}{(M+m)^2-\mu^2}\left[\frac{\alpha}{q^2}\right], \tag{1.4}$$

where M is the mass of the state, m and μ are nucleon and K-meson masses, respectively, and q is the center-of-mass momentum of the $\bar{K}$-N system at energy M. The constant α occurs in the imaginary part of the $J=\frac{3}{2}$ $\bar{K}$-N partial-wave amplitude: $\text{Im}f=(\pi/2)\alpha\delta(u^{1/2}-M)$. Here f is defined as $[\exp(2i\delta)-1]/2iq$ above the $\bar{K}$-N threshold, where δ is the complex phase shift for a state of definite isotopic spin. Above the $\bar{K}$-N threshold one has $\alpha=x\Gamma/q$, where Γ is the width of the resonance in energy units, and x is the fraction of decays into the $\bar{K}$-N channel. Below threshold α is a negative number which is no longer determined by the experimental parameters of the resonance. Thus, the coupling constants H^2 for $Y_0^*(1520 \text{ MeV})$ and $Y_1^*(1660 \text{ MeV})$ are determined by measured widths and branching ratios. The $Y_1^*(1385 \text{ MeV})$ lies below threshold, so there is no direct experimental access to its coupling strength. For the two resonances above threshold Eq. (1.4) yields the following coupling constants:

$$Y_0^*(1520 \text{ MeV}): \quad H^2/4\pi=0.41,$$
$$Y_1^*(1660 \text{ MeV}): \quad H^2/4\pi=0.17. \tag{1.5}$$

We have assumed that Y_0^* decays into $\bar{K}$-N 35% of the

[13] R. H. Dalitz and S. F. Tuan, Phys. Rev. Letters **3**, 425 (1960). For a discussion of the $\bar{K}$-N virtual bound state in the light of recent data, see R. H. Dalitz, Ref. 4.

[14] J. Schwinger, Phys. Rev. Letters **12**, 237 (1964).

[15] P. L. Connolly *et al.*, in Proceedings of the International Conference on High Energy Nuclear Physics, Dubna, U.S.S.R., 1964 (to be published).

[16] M. Taher-Zadeh, D. J. Prowse, P. E. Schlein, W. E. Slater, D. H. Stork and H. K. Ticho, Phys. Rev. Letters **11**, 470 (1963).

[17] W. E. Humphrey and R. R. Ross, Phys. Rev. **127**, 1305 (1962).

[18] Sakurai introduces $\boldsymbol{\tau}/2$ rather than $\boldsymbol{\tau}$ (cf. Ref. 34). Therefore his values for $\gamma_{\rho KK}\gamma_{\rho NN}{}^{(1)}$ are four times ours, by definition.

time ($x=0.35$).[19] We take $x=0.25$ for Y_1^* decays, although there is some experimental uncertainty about this number. Alvarez *et al.*[20] obtained $x<0.05$, while Bastien and Berge[21] found $x=0.25\pm0.10$ provided $J=\frac{3}{2}$. Smith *et al.*[22] report the branching ratios $\Lambda\pi:\Sigma\pi:\Lambda\pi\pi:\Sigma\pi\pi:\bar{K}N=7:6:1:(?):(>3)$. This uncertainty does not cause us much difficulty, since even if x is as large as 0.5 the contribution of Y_1^* exchange is quite minor.

The coupling constant for Y_0^*(1405 MeV) is determined approximately by the Y_0^* mass alone, if the Dalitz-Tuan model is assumed. In that model the $I=0$ s-wave $\bar{K}$-N amplitude f may be extrapolated below threshold by means of a constant complex scattering length. In the zero-width approximation for the resonance one finds

$$\operatorname{Im}f=(M|q|/E\omega)\pi\delta(u^{1/2}-M)\,, \tag{1.6}$$

where E and ω are the (unphysical) energies of N and $\bar{K}$, respectively, at the energy M of the resonance; q is the (unphysical) $\bar{K}$-N momentum at the energy M. By once more equating the pole residue appearing in the dispersion relation with that obtained from the Lagrangian, we have

$$Y_0^*(1405\text{ MeV}):\quad \frac{G^2}{4\pi}=\frac{M^2|q|}{E\omega}\frac{1}{E+m}=0.32\,. \tag{1.7}$$

The constant-scattering-length extrapolation may not be accurate because of the proximity of singularities due to exchange of light bosons.[23] Nevertheless, the estimate of Eq. (1.7) leads to such a small contribution to K-N scattering that variations of $\pm100\%$ about that estimate have no appreciable effect on our results. This circumstance is closely connected with the small magnitude of the terms from s-wave $\bar{K}$-N scattering, which has the quantum numbers of Y_0^*(1405 MeV).

For the coupling of Y_1^*(1385 MeV), we can only obtain an estimate based on $SU(3)$ symmetry.[24] It seems rather certain[25] that Y_1^*(1385 MeV) belongs to the (3,0) decuplet representation of $SU(3)$, along with $N_{3/2}^*$(1238 MeV), $\Xi_{1/2}^*$(1530 MeV), and Ω_0(1686±12 MeV).[26] By assuming that the decuplet-baryon-meson coupling constants $H_{B^*BP}^2$ have ratios given by strict $SU(3)$ symmetry, one can calculate $H_{Y_1^*NK}^2$ from the known width of $N_{3/2}^*$. The result is

$$Y_1^*(1385\text{ MeV}):\quad H^2/4\pi=2.4\,. \tag{1.8}$$

In general, one expects large symmetry breaking in the decuplet, and the prediction of coupling-constant ratios on the basis of strict symmetry is risky. An idea of what to expect may be obtained from a specific model of the broken decuplet by Wali and Warnock.[25] The model agrees well with most observations and satisfies the coupling-constant sum rules of Gupta and Singh.[27] It yields the value

$$Y_1^*(1385\text{ MeV}):\quad H^2/4\pi=1.9\,. \tag{1.9}$$

We employ Eq. (1.9) in our calculations.

The above estimates of the four Y^* coupling constants may not be extremely accurate, but it turns out that they are quite sufficient for our purposes. In Sec. II we show that the interesting parameters that we try to determine by data fitting (e.g., the ρ coupling constant) are highly insensitive to the Y^* constants. In fact, one can omit the four Y^* terms entirely, without great changes in the best-fit values of the free parameters. This is true in spite of the fact that one of these terms [Y_0^*(1520 MeV)] is not particularly small.

Very little is known about the $KN\Lambda$ and $KN\Sigma$ coupling constants, in spite of the fact that the problem of their determination has existed for a long time. The best we can do is calculate these constants from $SU(3)$ and the known value of the πNN coupling. Even this does not yield unique values, since the ratio of D- and F-type[24] meson-baryon couplings is uncertain. Martin and Wali[28] have determined a range for this ratio on the basis of a single-baryon exchange model. In terms of their D-F mixing parameter f, they find $0.15<f<0.55$. Since $G_{KN\Lambda}^2=\frac{1}{3}(1+2f)^2G_{\pi NN}^2$ and $G_{KN\Sigma}^2=(1-2f)^2\times G_{\pi NN}^2$, an f in this range implies

$$\begin{aligned}&8.4<G_{KN\Lambda}^2/4\pi<22\,,\\&7.3>G_{KN\Sigma}^2/4\pi>0.15\,.\end{aligned} \tag{1.10}$$

We have taken $G_{\pi NN}^2/4\pi$ to be 15. The large value of $G_{KN\Lambda}$ implied by (1.10) has been regarded with some suspicion, since it was thought that the K-meson couplings were significantly weaker than the pion couplings. However, the K coupling strengths were estimated by comparing the Born approximation for K-hyperon photoproduction with experiment.[29] It now seems likely that this kind of estimate is much too crude. A recent experiment of Peck[30] on $\gamma+p\rightarrow K_++\Lambda$ at 1200 MeV was intended to measure the $KN\Lambda$ coupling constant, but resulted in no conclusion at all about its value. Peck attempted an extrapolation in $\cos\theta$ to the K-meson exchange pole, following a method used successfully to detect the pion pole and to measure

---

[19] M. Ferro-Luzzi, R. D. Tripp, and M. B. Watson, Phys. Rev. Letters **8**, 28 (1962).

[20] L. W. Alvarez, M. H. Alston, M. Ferroluzzi, D. O. Huwe, G. R. Kalbfleisch, *et al.*, Phys. Rev. Letters **10**, 184 (1963).

[21] P. L. Bastien and J. P. Berge, Phys. Rev. Letters **10**, 188 (1963).

[22] G. A. Smith *et al.*, *Proceedings of the Conference on Recently Discovered Resonant Particles*, Ohio University, Athens, Ohio, 1963 (unpublished).

[23] R. H. Dalitz, Rev. Mod. Phys. **33**, 471 (1961); see especially Sec. IV.

[24] M. Gell-Mann, Phys. Rev. **125**, 1067 (1962); California Institute of Technology Report CTSL-20, 1961 (unpublished); Y. Ne'eman, Nucl. Phys. **26**, 222 (1961).

[25] K. C. Wali and R. L. Warnock, Phys. Rev. **135**, B1358 (1964).

[26] V. E. Barnes, P. L. Connolly, D. J. Crennell, B. B. Culwick, W. C. Delaney, *et al.*, Phys. Rev. Letters **12**, 204 (1964).

[27] V. Gupta and V. Singh, Phys. Rev. **135**, B1442 (1964).

[28] A. W. Martin and K. C. Wali, Phys. Rev. **130**, 2455 (1963).

[29] M. Gell-Mann, Phys. Rev. **106**, 1296 (1957).

[30] C. W. Peck, Phys. Rev. **135**, B830 (1964).

its residue in $\gamma+p\rightarrow\pi_{+}+n$.[31] The accuracy of the data turned out to be inadequate for such a long extrapolation. Also, the data show no evidence for the presence of the pole. Cook *et al.*[32] have attempted to determine an average of the Λ and Σ residues in the forward-angle dispersion relations for K-N and $\bar{K}$-N scattering. This method also yields little information. The result of Cook *et al.* for the average of the two couplings is

$$(G^2/4\pi)_{\mathrm{av}}=2.6\pm7.0. \qquad (1.11)$$

If we suppose that $G_{KN\Sigma}{}^2$ is negligible with respect to $G_{KN\Lambda}{}^2$, as is nearly the case in the $SU(3)$ scheme for the popular value $f=0.35$ of the D-F mixing parameter, then Eq. (1.11) implies $0<G_{KN\Lambda}{}^2/4\pi<19$.

For the coupling constants of the t-channel states, there is no information that can be taken directly from existing experiments. But if we assume that the ρ dominates the nearby singularities of the nucleon isovector electromagnetic form factor, we may calculate the ratio $\gamma^{(2)}/\gamma^{(1)}$ of tensor to vector $\bar{N}N\rho$ couplings. This procedure was followed by Bowcock, Cottingham, and Lurié in their treatment of π-N scattering.[2] According to the isovector-form-factor fit of de Vries, Hofstadter, and Herman,[33] which involves only a ρ-meson pole and a subtraction constant, the ratio is given by

$$\gamma^{(2)}/\gamma^{(1)}=4.4. \qquad (1.12)$$

We have employed Eq. (1.12) throughout our work.

The coupling constant product $\gamma_{KK\rho}\gamma_{NN\rho}{}^{(1)}$ may be estimated from $SU(3)$ invariance, if we note that $\gamma_{NN\rho}{}^{(1)}$ has already been estimated by obtaining $\gamma_{\pi\pi\rho}$ from the ρ width, and $\gamma_{\pi\pi\rho}\gamma_{NN\rho}{}^{(1)}$ from isospin-dependent s-wave π-N scattering. Sakurai[34] finds $\gamma_{NN\rho}{}^{(1)2}/4\pi\approx\gamma_{\pi\pi\rho}{}^2/4\pi\approx0.55$; since $\gamma_{KK\rho}=\gamma_{\pi\pi\rho}$ according to $SU(3)$, we have also

$$\gamma_{KK\rho}\gamma_{NN\rho}{}^{(1)}/4\pi\approx0.55. \qquad (1.13)$$

For the coupling constants involved in the φ and ω exchange terms, no estimates can be made from $SU(3)$ invariance alone. In fact, in the picture of φ-ω mixing,[35] one would have to know the φ-ω mixing angle λ, the D-F ratio for coupling of the octuplet of vector mesons to the baryons, and the strength of coupling of the singlet vector meson to the baryons. Although the mixing angle may be estimated roughly, we know nothing about the other parameters. We are therefore faced with the four free parameters $\gamma_{KK\omega}\gamma_{NN\omega}{}^{(1,2)}$, $\gamma_{KK\varphi}\gamma_{NN\varphi}{}^{(1,2)}$. As we mentioned earlier, the K-N scattering data do not appreciably constrain coupling constants of $I=0$, t-channel states. This means that there is no hope of determining the four constants associated with φ and ω by means of present data. In an attempt to make the best of this situation, we have tried to represent both the φ and ω exchanges by the exchange of a single vector meson with mass equal to the root mean square of φ and ω masses. The fictitious meson is denoted by χ. Representation of both φ and ω by χ would not be a good approximation if the data fits were at all sensitive to what goes on in the $I=0$ t channel. This may be seen from the tables in Sec. III, which show that φ exchange terms decrease a good deal more rapidly with orbital angular momentum than ω exchange terms. We find, however, that even the two constants $\gamma_{\chi KK}\gamma_{\chi NN}{}^{(1,2)}$ are not well determined in the data fits. This leads us to believe that lumping of the φ and ω terms is not too grave an error. As a check, we have also performed fits with separate φ and ω terms; the results are discussed in the following section. One can make a guess at the constant $\gamma_{\chi KK}\gamma_{\chi NN}{}^{(1)}$ on the basis of $SU(3)$ and the φ-ω mixing theory. The physical φ and ω are written as linear combinations of the almost-pure octet state $\varphi^{(0)}$ and the almost-pure singlet state $\omega^{(0)}$.

$$\varphi=(\cos\lambda)\varphi^{(0)}+(\sin\lambda)\omega^{(0)}$$
$$\omega=-(\sin\lambda)\varphi^{(0)}+(\cos\lambda)\omega^{(0)}.$$

Since $\omega^{(0)}$ does not couple to a pair of pseudoscalar mesons in the pure-symmetry limit, we have the following approximate expressions for the φ and ω coupling constants.

$$\gamma_{\varphi KK}\gamma_{\varphi NN}=(\cos\lambda)\gamma_{\varphi^{(0)}KK}\times[(\cos\lambda)\gamma_{\varphi^{(0)}NN}+(\sin\lambda)\gamma_{\omega^{(0)}NN}],$$
$$\gamma_{\omega KK}\gamma_{\omega NN}=(\sin\lambda)\gamma_{\varphi^{(0)}KK}\times[(\sin\lambda)\gamma_{\varphi^{(0)}NN}-(\cos\lambda)\gamma_{\omega^{(0)}NN}].$$

If M_x denotes the matrix element for exchange of meson x, then the sum of φ and ω exchange terms may be written

$$\gamma_{\varphi^{(0)}KK}\gamma_{\varphi^{(0)}NN}M_\chi+\gamma_{\varphi^{(0)}KK}\gamma_{\varphi^{(0)}NN}\times[(\cos^2\lambda)(M_\varphi-M_\chi)+(\sin^2\lambda)(M_\omega-M_\chi)]+(\sin\lambda\cos\lambda)\gamma_{\varphi^{(0)}KK}\gamma_{\omega^{(0)}NN}(M_\varphi-M_\omega). \qquad (1.14)$$

Provided $\gamma_{\omega^{(0)}NN}$ is not too large, the first term of Eq. (1.14) should be dominant, since the other terms are proportional to mass differences. Thus, when we have only χ exchange we may suppose that $\gamma_{\chi KK}\gamma_{\chi NN}$ is roughly equal to $\gamma_{\varphi^{(0)}KK}\gamma_{\varphi^{(0)}NN}$. Needless to say, this is an exceedingly crude estimate. If the gauge theory holds, so that vector mesons are coupled to baryons by pure-F

[31] R. L. Walker, *Proceedings of the Tenth Annual International Conference on High Energy Physics at Rochester*, 1960 (Interscience Publishers, Inc., New York, 1960), p. 17.

[32] V. Cook, D. Keefe, L. T. Kerth, P. G. Murphy, W. A. Wenzel, and T. F. Zipf, Phys. Rev. **129**, 2743 (1963).

[33] C. de Vries, R. Hofstadter, and R. Herman, Phys. Rev. Letters **8**, 381 (1962); and two errata: *ibid.* **8**, 466 (1962); and **9**, 414 (1962).

[34] J. J. Sakurai, *Theoretical Physics*, International Atomic Energy Agency, Vienna, 1963 (Lectures presented at the Seminar on Theoretical Physics organized by the International Atomic Energy Agency, Palazzino Miramare, Trieste, July–August, 1962); *Proceedings of the International School of Physics "Enrico Fermi," Course 26* (Academic Press Inc., New York, 1963).

[35] S. Okubo, Phys. Letters **5**, 165 (1963); J. J. Sakurai, Phys. Rev. **132**, 434 (1963); S. L. Glashow, Phys. Rev. Letters **11**, 48 (1963); R. F. Dashen and D. H. Sharp, Phys. Rev. **133**, B1585 (1964); Y. S. Kim, S. Oneda, and J. C. Pati, *ibid.* **135**, B1076 (1964).

vector couplings, one has $\gamma_{\varphi^{(0)}NN}^{(1)}=\sqrt{3}\gamma_{\rho NN}^{(1)}$. Since also $\gamma_{\varphi^{(0)}KK}=\sqrt{3}\gamma_{\rho\pi\pi}$, Eq. (1.13) and the above assumptions lead to

$$\gamma_{XKK}\gamma_{XNN}^{(1)}\approx 3(\gamma_{\rho\pi\pi}\gamma_{\rho NN}^{(1)}/4\pi)\approx 1.6. \quad (1.15)$$

This completes our survey of present knowledge of coupling constants. Before proceeding to the data fitting, the effects of the unitarity requirement must be examined. The single-particle exchange terms and the background terms of Eq. (1.2) are real functions at physical energies. Unitarity requires that the scattering amplitude have an imaginary part, so we must discuss the integral over the physical branch cut which produces the imaginary part. In principle, this integral may be evaluated from experimental data, but the data available are actually quite inadequate to the task. Nevertheless, one can estimate an upper bound for the integral, and in Sec. IV we do so. We estimate that at the highest momentum of our fits (810 MeV/c in the laboratory) the real parts of the integrals represent at most 10% of the experimental values of the real parts of the partial-wave amplitudes. At the lower momenta the integrals are proportionately smaller. Although corrections of this magnitude are not strictly negligible, they will not change our qualitative conclusions, and will cause fairly minor changes in quantitative conclusions. In our main discussion of data fitting in Sec. II we omit the unitarity integrals, since we have no reason to believe any precise assumption about their behavior. In Sec. IV we carry out data fits including some "sample" unitarity integrals, in order to give some indication of the quantitative changes that unitarity may bring about.

II. DATA FITTING AND COMPARISON OF FITS WITH THEORETICAL PREDICTIONS

In the $I=1$ state we fit phase shifts determined by Goldhaber *et al.*[36] from their K_+-p bubble-chamber data at eight laboratory momentum values between 140 and 642 MeV/c. These data indicate that the K_+-p interaction is pure s wave, with a negative phase shift, up to 642 MeV/c. We also include in our fits an $I=1$ phase shift at 810 MeV/c as determined by Stubbs *et al.*[37] There are some ambiguities in the phase-shift analysis at 810 MeV/c, but only one of the phase-shift sets joins in a reasonable way with the phases for lower momenta. Also, arguments against some of the other phase-shift sets are given in Ref. 37. The set we choose is the one labeled A^- in Ref. 37. It corresponds again to a dominant s wave with negative phase shift. The associated p waves are quite small: $\delta(P_{1/2})=0.5°\pm4.5°$, $\delta(P_{3/2})=1.5°\pm4.5°$. The remarkable dominance of s waves up to 810 MeV/c is a powerful constraint on the parameters of our theory. In making our fits we have set the p and d waves equal to zero, within assigned errors, at 355, 520, 642, and 810 MeV/c. The errors are shown in Figs. 2(b), 2(c), 3(b), and 3(c); they represent what we think is a liberal guess at the maximum tolerable amounts of p and d waves. Note that the graphs in Figs. 2 and 3 are of $q\,\mathrm{Re}f=\sin\delta\cos\delta$, the quantity to which our theoretical amplitudes are to be compared. The errors of all of the $I=1$ data shown in Figs. 2 and 3 are treated as uncorrelated.

In the $I=0$ state we employ phase shifts computed by Stenger and collaborators[38] from deuterium bubble-chamber data on the reactions

$$K_++d\rightarrow K_0+p+p\,,$$
$$K_++d\rightarrow K_++d\,,$$
$$K_++d\rightarrow K_++n+p\,.$$

Stenger *et al.* have found phase shift fits involving s and p waves only, and also fits with s, p, and d waves, at 350, 530, 642, and 812 MeV/c. With reasonable values of the coupling constants, our theory indicates substantial d waves at the higher momenta, barring "accidental" cancellations of the type that seem to occur in $I=1$. For this reason we have used the s, p, d phase shift sets. There are two sets, corresponding to the Fermi-Yang ambiguity. They are shown in Figs. 2d–2h and 3d–3h, in terms of $\sin\delta\cos\delta$.[39] The Fermi-type set [$\delta(P_{1/2})$ large and positive] is labeled SPD-1, while the Yang-type set [$\delta(P_{1/2})$ large and positive] is called SPD-2. The errors are strongly correlated, so the phase shifts are more strongly constrained than the diagonal error matrix elements shown in the figure would lead one to believe. The error matrix given in Ref. 38 has been incorporated in χ^2 fits of our theory to the data.

We shall not discuss the theoretical uncertainties involved in using the impulse approximation to extract the $I=0$ phase shifts from the K_+-d data. These questions are treated in Ref. 38. One hopes that eventually a $K_2{}^0$ beam can be used to gather directly accurate information on the $I=0$ interaction.

We make a χ^2 fit to the 45 pieces of data shown in Figs. 2 or 3. Because of the large number of degrees of freedom and the correlations of errors in the $I=0$ phase shifts, the computation of χ^2 requires a great number of arithmetic operations. Because of the consequent round-off error we found it necessary to use double precision arithmetic on the IBM 7090 computer; that amounts to carrying approximately 16 significant figures. The prob-

[36] S. Goldhaber, W. Chinowsky, G. Goldhaber, W. Lee, T. O'Halloran *et al.*, Phys. Rev. Letters **9**, 135 (1962).

[37] T. F. Stubbs, H. Bradner, W. Chinowsky, G. Goldhaber, W. Slater, D. M. Stork, H. K. Ticho, Phys. Rev. Letters **7**, 188 (1961).

[38] V. J. Stenger, W. E. Slater, D. H. Stork, H. K. Ticho, G. Goldhaber, and S. Goldhaber, Phys. Rev. **134**, B1111 (1964).

[39] The treatment of errors at the two highest momentum points of Fig. 3(e) requires some explanation. Here the phase shifts are almost 45°, so $\sin\delta\cos\delta$ is near its maximum. Therefore, the uncertainty in $\sin\delta\cos\delta$ is entirely in the downward direction. For the χ^2 fitting procedure and for the error bars of Fig. 3(e) we have taken the standard deviation to be one-half the downward uncertainty. This amount of constraint in the upward direction does not prevent the theoretical curve from overshooting slightly the unitarity limit.

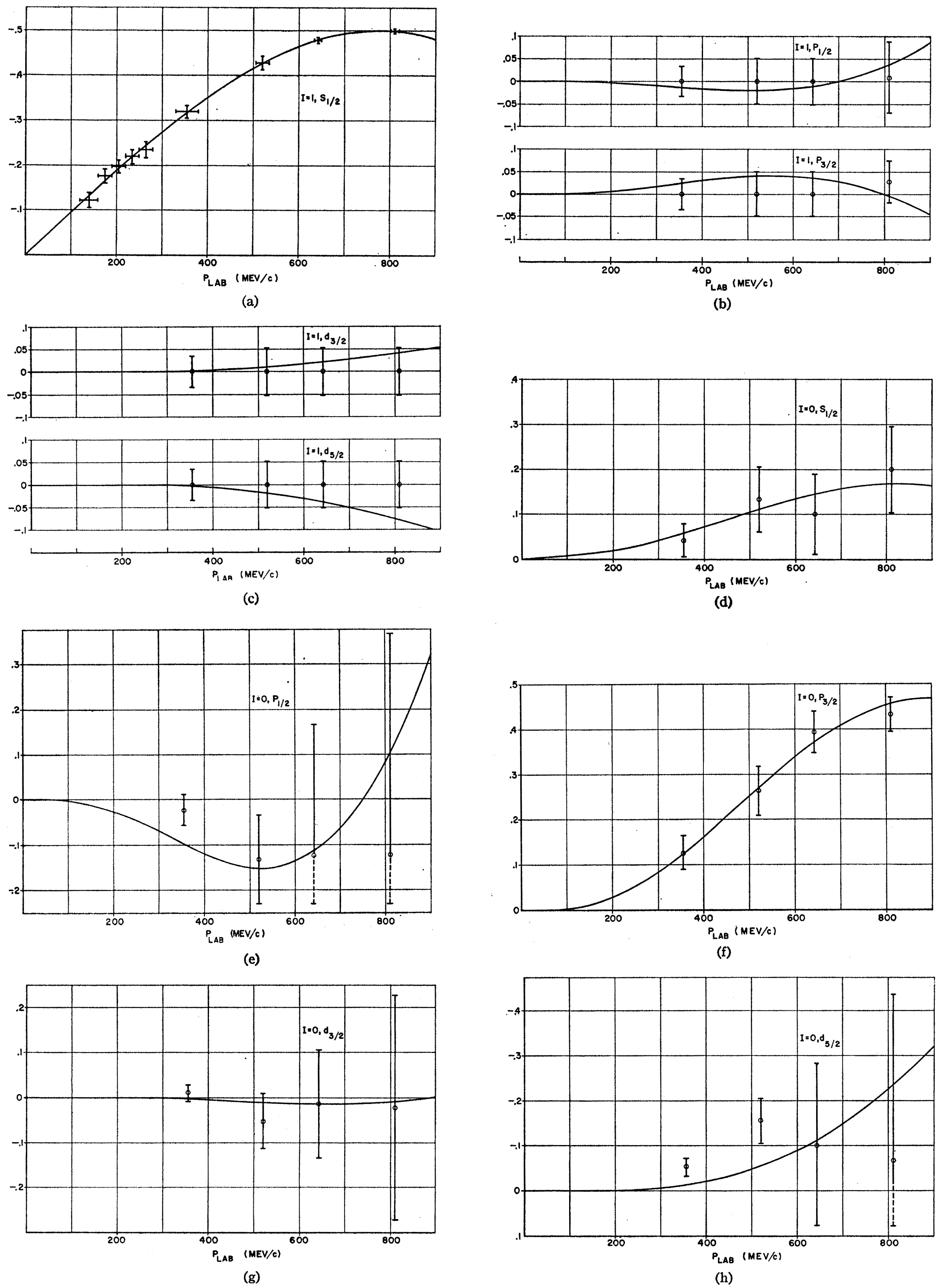

FIG. 2. Data and theoretical curves for fit 1-B of Table II. The $I=0$ data are from the Fermi-type phase-shift set SPD-1 of Stenger *et al.* (Ref. 38). The quantity plotted is q Re$f=\sin\delta\cos\delta$, where δ is the phase shift.

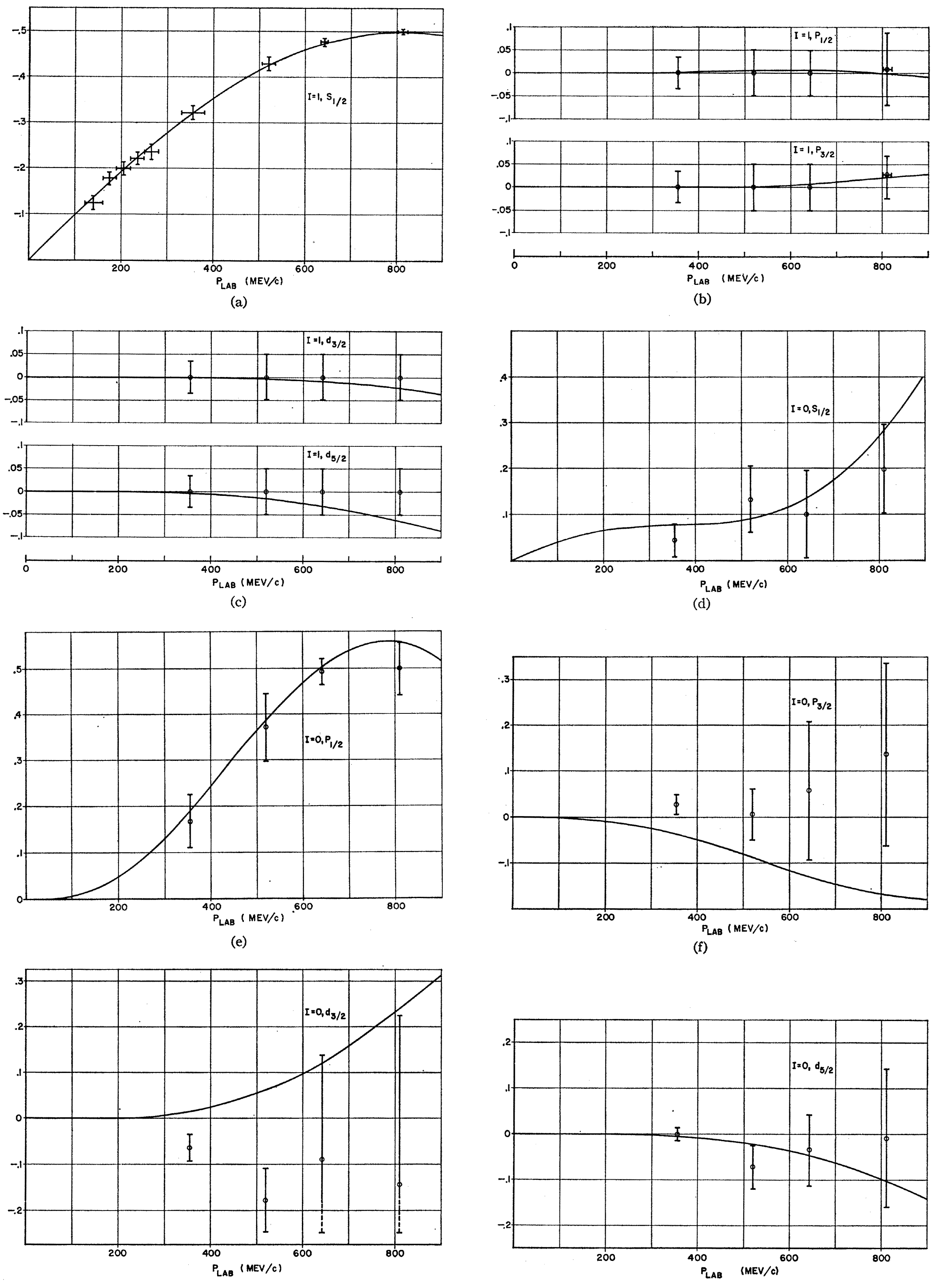

FIG. 3. Data and theoretical curves for fit 2-*B* of Table IV. The $I=0$ data are from the Yang-type phase-shift set SPD-2 of Stenger *et al.* (Ref. 38). The quantity plotted is $q\ \mathrm{Re}f=\sin\delta\cos\delta$, where δ is the phase shift.

lem was transferred later to the CDC 3600, which carries about 25 significant figures in double precision. The results from the two computers were identical, which proved that the trouble with round-off error had been cured.

We first tried a fitting procedure based on a minimal representation of the background due to short-range forces. This corresponds to keeping only the two parameters $\alpha^{(0)}$, $\alpha^{(1)}$ out of the eight parameters of Eq. (1.2). By computing a single-particle exchange term in the limit of infinite exchanged mass, one can see that this means a strictly zero-range background. Besides the two $\alpha^{(I)}$, we allowed the seven free parameters $G_{KN\Lambda}^2$, $G_{KN\Sigma}^2$, $\gamma_{\rho NN}^{(1)}$, $\gamma_{\chi NN}^{(1)}$, $\gamma_{\chi NN}^{(2)}$. As explained in Sec. I, χ represents the average effect of φ and ω. The two Y_0^*'s and the two Y_1^*'s were included with coupling constants given by Eqs. (1.5), (1.7), and (1.8). The resulting seven parameter amplitude could not be fitted to the forty-five pieces of data with an acceptable χ^2. The χ^2 values were extremely large: for phase shifts SPD-1, $\chi^2=344$, and for SPD-2, $\chi^2=401$. Also, it does not help to take separate φ and ω terms and ABC and K_1-K_1 exchanges. In that case we have eleven free parameters and $\chi^2=195$ (SPD-1), $\chi^2=327$ (SPD-2). It seems clear that the pattern of forces in K-N scattering is really quite complicated. This raises some doubt about earlier work in which only part of the data was fitted, and without estimates of the statistical significance of fits. The comparison of our calculations with earlier work is discussed further in Sec. VI.

The next systematic approximation for the background forces involves $\alpha^{(I)}$ and $\beta^{(I)}$. Allowing these four parameters and five free coupling constants $[\Lambda,\Sigma,\rho,\chi^{(1)},\chi^{(2)}]$ we find that the fits are still not satisfactory: $\chi^2=81$ (SPD-1), $\chi^2=305$ (SPD-2). Passing to the next approximation by adding $\alpha_s^{(I)}$ and $\alpha_t^{(I)}$, we find the good fits reported in the following. If only $\alpha_s^{(I)}$ or $\alpha_t^{(I)}$ terms are added, the fits are on the borderline of acceptability, but are not very good. With $\alpha_s^{(I)}$ only, $\chi^2=69$ (SPD-1), $\chi^2=62$ (SPD-2); with $\alpha_t^{(I)}$ only, $\chi^2=70$ (SPD-1), $\chi^2=65$ (SPD-2). One might argue that the α_t term is of higher order than the α_s term in the sense that the former contributes to $J=\frac{3}{2}$ states, while the latter does not (cf. the Appendix). In that case one might consider stopping the expansion at $\alpha_s^{(I)}$. However, it should not be forgotten that the data are very poor in some of the $I=0$ states; with better data we should almost certainly have to go beyond $\alpha_s^{(I)}$ to get acceptable fits. With present data it does not seem wise to improve borderline fits by allowing separate ω and φ parameters. In all such fits the χ coupling constants are already badly determined.

A. Phase Shifts SPD-1

We discuss first the fits to the Fermi-type phase shifts SPD-1. Table II shows the parameter values obtained in a series of fits corresponding to different hypotheses about the single-particle exchange terms. The parameters are constrained more than the diagonal error matrix elements indicate, since there are some strong error correlations. To illustrate, we list the correlation coefficients for fit 1-A in Table III. The fits labeled 1-B, 1-C, 1-E, 1-F, and 1-G all have $G_{KN\Lambda}=0$. The vanishing of $G_{KN\Lambda}$ is a result of applying the constraints $G_{KN\Lambda}^2\geqslant 0$, $G_{KN\Sigma}^2\geqslant 0$. The unconstrained best fits re-

TABLE II. Parameter values of fits with Fermi-type phase shifts SPD-1. A dash indicates that the term in question was not included in the fit. The 0^+ notation means that the best-fit value of the parameter was zero, because of the constraint $G^2\geqslant 0$ (see text). The asterisk indicates that the parameter value given was taken as input. Fit 1-G is like fit 1-B, except that it omits the Y^* terms.

	Fits with phase shifts SPD-1							
		1-A	1-B	1-C	1-D	1-E	1-F	1-G
	χ^2	28	35	76	141	47	34	39
	$P(\chi^2)$	0.98	0.85	<0.005	<0.005	0.41	0.88	0.72
	Best-fit values of parameters							
1	$G_{KN\Lambda}^2/4\pi$	-38 ± 14	0^+	0^+	14.4*	0^+	0^+	0^+
2	$G_{KN\Sigma}^2/4\pi$	51 ± 9	58 ± 9	$\cdots$	1.3*	60 ± 8	57 ± 9	56 ± 9
3	$\gamma_\rho NN^{(1)}\gamma_\rho KK/4\pi$	-0.46 ± 0.20	-0.54 ± 0.20	-0.86 ± 0.19	0.55*	$\cdots$	-0.44 ± 0.21	-0.54 ± 0.20
4	$\gamma_\chi NN^{(1)}\gamma_\chi KK/4\pi$	3.8 ± 3.2	3.1 ± 3.2	-2.3 ± 3.0	4.0 ± 2.0	$\cdots$	3.3 ± 3.2	4.8 ± 3.2
5	$\gamma_\chi NN^{(2)}\gamma_\chi KK/4\pi$	-4.0 ± 5.1	-3.4 ± 5.1	6.7 ± 4.8	-2.3 ± 4.7	$\cdots$	-1.1 ± 6.7	6.5 ± 5.1
	$gh/4\pi$ (ABC)	$\cdots$	$\cdots$	$\cdots$	$\cdots$	$\cdots$	-0.15 ± 0.15	$\cdots$
	$gh/4\pi$ (K_1-K_1)	$\cdots$	$\cdots$	$\cdots$	$\cdots$	$\cdots$	12 ± 10	$\cdots$
6	$\alpha^{(1)}$	-6 ± 38	86 ± 17	-8.4 ± 8.7	23 ± 9	102 ± 16	71 ± 22	80 ± 17
7	$\alpha^{(0)}$	340 ± 50	301 ± 48	4 ± 12	-80 ± 8	303 ± 48	277 ± 52	290 ± 48
8	$\alpha_s^{(1)}$	0.23 ± 0.30	-0.44 ± 0.18	0.02 ± 0.16	-0.14 ± 0.16	-0.69 ± 0.11	-0.51 ± 0.22	-0.35 ± 0.18
9	$\alpha_s^{(0)}$	-2.2 ± 0.4	-1.9 ± 0.3	-0.21 ± 0.21	1.0 ± 0.1	-1.9 ± 0.3	-1.9 ± 0.3	-1.8 ± 0.3
10	$\alpha_t^{(1)}$	0.47 ± 0.33	-0.22 ± 0.20	0.14 ± 0.20	0.26 ± 0.19	-0.46 ± 0.11	-0.43 ± 0.27	-0.37 ± 0.21
11	$\alpha_t^{(0)}$	-2.1 ± 0.4	-1.8 ± 0.3	0.01 ± 0.21	0.70 ± 0.19	-2.1 ± 0.3	-1.9 ± 0.4	-1.4 ± 0.3
12	$\beta^{(1)}$	-1.1 ± 3.3	6.2 ± 2.0	-1.7 ± 1.5	4.1 ± 1.5	8.4 ± 1.3	7.4 ± 2.6	5.9 ± 2.0
13	$\beta^{(0)}$	30 ± 4	27 ± 4	4.3 ± 2.3	-11 ± 1	24 ± 4	27 ± 4	27 ± 4

TABLE III. Matrix of error correlation coefficients for fit 1-A of Table II.

	1	2	3	4	5	6	7	8	9	10	11	12	13
1	1	0.26	−0.14	−0.08	0.04	0.89	−0.28	−0.81	0.26	−0.78	0.27	0.80	−0.25
2		1	0.21	0.24	−0.28	0.61	0.83	−0.44	−0.67	−0.37	−0.68	0.57	0.72
3			1	0.35	−0.32	−0.03	0.11	0.09	0.16	0.21	−0.04	0.11	−0.15
4				1	−0.76	−0.11	0.12	0.37	0.18	0.55	0.29	0.03	0.12
5					1	0.13	−0.10	−0.46	−0.25	−0.50	−0.22	0.20	0.04
6						1	0.16	−0.93	−0.17	−0.88	−0.17	0.94	0.15
7							1	−0.09	−0.92	−0.06	−0.91	0.16	0.94
8								1	0.21	0.97	0.23	−0.91	−0.12
9									1	0.22	0.95	−0.16	−0.95
10										1	0.26	−0.78	−0.07
11											1	−0.14	−0.84
12												1	0.18
13													1

sulted in $G_{KN\Lambda}^2<0$. It follows that the constrained best fits have $G_{KN\Lambda}=0$. This is because χ^2 is a bilinear, inhomogeneous function of the parameters, and thus has only one extremum, which is a minimum. χ^2 must increase monotonically with the distance from the minimum point. Label the parameters $(\lambda_1,\lambda_2,\cdots\lambda_n)$ and suppose that the unconstrained best fit is at the point $\boldsymbol{\lambda}^0=(\lambda_1{}^0,\lambda_2{}^0,\cdots\lambda_n{}^0)$, where $\lambda_1{}^0<0$. Suppose that the constrained best fit is at $\boldsymbol{\lambda}^1=(\lambda_1{}^1,\lambda_2{}^1,\cdots\lambda_n{}^1)$. It is clear that $\lambda_1{}^1=0$, because if $\lambda_1{}^1>0$ then the point $\boldsymbol{\lambda}^2=(0,\lambda_2{}^1,\cdots\lambda_n{}^1)$ lies closer to $\boldsymbol{\lambda}^0$ than $\boldsymbol{\lambda}^1$ does. Similarly, if there are several negative parameters in the unconstrained best fit, say $\lambda_1<0$, $\lambda_2<0$, $\cdots$, $\lambda_k<0$, then the best fit subject to the requirements $\lambda_1\geqslant 0$, $\lambda_2\geqslant 0$, $\cdots$, $\lambda_n\geqslant 0$ involves $\lambda_1=\lambda_2=\cdots=\lambda_k=0$.

The fit 1-A, listed first in Table II, is given as an example of an unconstrained fit leading to a negative G^2; viz., $G_{KN\Lambda}^2/4\pi=-38\pm 14$. Fit 1-$B$ is similar to 1-A, except that $G_{KN\Lambda}$ is set to zero. It is interesting that the Σ, ρ, and χ couplings are rather similar in these two fits, despite the large change in $G_{KN\Lambda}$. This marked insensitivity of the Σ, ρ, and χ terms to the Λ coupling constants is illustrated also by the matrix of correlation coefficients given in Table III, which shows that Λ-Σ, Λ-ρ, and Λ-χ correlations are relatively weak. We have $C_{\Lambda\text{-}\Sigma}=C_{12}=0.26$, $C_{\Lambda\text{-}\rho}=C_{13}=-0.14$, $C_{\Lambda\text{-}\chi(1)}=C_{14}=-0.08$, $C_{\Lambda\text{-}\chi(2)}=C_{15}=0.04$. Table III is informative in other respects. For example, it shows that Λ and Σ correlate strongly with the background terms, but weakly with the vector meson exchange terms. This is no surprise, since we know that the Λ and Σ exchanges correspond to forces of very short range, as do the background terms. On the other hand, the ρ and φ-ω exchanges may produce the most important long-range forces of the problem. The tensor and vector χ exchange terms are strongly correlated: $C_{\chi(1)\text{-}\chi(2)}=C_{45}=-0.76$.

The relatively small error for the Σ coupling constant $G_{KN\Sigma}^2$ in fit 1-B suggests that the Σ term is essential to the fit. This is confirmed by fit 1-C, in which Σ is dropped, but the other terms included are the same as in fit 1-B. The χ^2 rises to an unacceptable value. Apparently the main role of the Σ term is to produce the strong attraction in the $I=0$, $P_{3/2}$ state which is characteristic of phase shifts SPD-1. Here we are dealing with the same sort of force that is thought to be mainly responsible for $N_{3/2}{}^*(1238\text{ MeV})$. The ratio of the Σ contributions to the two isospin states is $3(I=0):1(I=1)$, so given the possibility of cancellation with background in $I=1$, the Σ can produce the desired effect.

The ρ term is much less essential in the fits than Σ, although it shares with Σ the property of having a coupling constant that is relatively stable to changes in other terms. In fit 1-E we omit the vector mesons entirely and the fit remains good. The χ terms, particularly, seem to play no significant role. According to fit 1-B the χ coupling constants may be taken to vanish within the errors, and the errors are huge.

In fit 1-B both the Σ and ρ coupling constants differ by about five and one-half standard deviations from the $SU(3)$ predictions of Eq. (1.10) and Eq. (1.13). Since the ρ term is not very important to the fit, the most serious discrepancy is the disagreement of $G_{KN\Sigma}^2$ with Eq. (1.10). Of course, Eq. (1.10) is not a prediction of $SU(3)$ invariance alone; it was derived from the single-baryon exchange model plus the assumption that $\frac{3}{2}^+$ meson-baryon resonances occur only in the 10 representation. Nevertheless, a phenomenological study of hyperfragment data by Dalitz[40] yielded a D-F mixing parameter in the range corresponding to Eq. (1.10). We should be surprised if Eq. (1.10) were strongly contradicted. This leads us to the conclusion that the phase shift set SPD-1 is probably not the correct one. Even without bringing in $SU(3)$ arguments it seems difficult to accept phases SPD-1, since the implied large value of $G_{KN\Sigma}^2$ would probably be very hard to reconcile with data on Σ photo production.[41] This value also does not agree with the result from forward-angle dispersion relations, Eq. (1.11).

In fit 1-D we take as input some "$SU(3)$ values" for the Λ, Σ, and ρ coupling constants. Specifically, the ρ constant is given the value of Eq. (1.13) and the Λ and Σ constants the values corresponding to 0.35 for the mixing parameter f and 15 for $G_{\pi NN}^2/4\pi$. The χ^2 of run

[40] R. H. Dalitz, Phys. Letters **5**, 53 (1963).
[41] J. Dufour, Orsay report (unpublished).

TABLE IV. Parameter values of fits with Yang-type phase shifts SPD-2. Notation is explained in the caption of Table II.

		Fits with phase shifts SPD-2						
		2-*A*	2-*B*	2-*C*	2-*D*	2-*E*	2-*F*	2-*G*
	χ^2	52	55	64	94	87	49	54
	$P(\chi^2)$	0.27	0.16	0.034	<0.005	<0.005	0.32	0.094
		Best-fit values of parameters						
1	$G_{KN\Lambda}^2/4\pi$	13±16	7±16	14.4*	59±13	15±15	3±17	−2±16
2	$G_{KN\Sigma}^2/4\pi$	−24±14	0^+	1.3*	0^+	0^+	0^+	0^+
3	$\gamma_\rho NN^{(1)}\gamma_\rho KK/4\pi$	0.62±0.23	0.92±0.15	0.52*	···	1.2±0.1	0.88±0.15	1.0±0.15
4	$\gamma_\chi NN^{(1)}\gamma_\chi KK/4\pi$	6.1±3.4	4.8±3.4	1.3±3.1	−0.3±1.9	···	4.6±3.4	6.1±3.4
5	$\gamma_\chi NN^{(2)}\gamma_\chi KK/4\pi$	−20±5	−21±5	−22±5	−23±4	···	−23±7	−24±5
	$gh/4\pi$ (ABC)	···	···	···	···	···	−0.19±0.15	···
	$gh/4\pi$ (K_1-K_1)	···	···	···	···	···	10±11	···
6	$\alpha^{(1)}$	−58±38	−26±33	−13±9	71±29	32±31	−49±38	−47±33
7	$\alpha^{(0)}$	−225±92	−80±35	−76±11	−167±32	−62±32	−86±39	−58±35
8	$\alpha_s^{(1)}$	0.76±0.30	0.53±0.27	0.47±0.17	−0.07±0.26	−0.34±0.22	0.62±0.37	0.72±0.27
9	$\alpha_s^{(0)}$	2.0±0.63	1.1±0.3	0.93±0.19	1.5±0.3	0.58±0.22	1.0±0.3	1.0±0.3
10	$\alpha_t^{(1)}$	1.0±0.3	0.77±0.30	0.52±0.21	−0.16±0.26	0.04±0.23	0.70±0.43	0.72±0.30
11	$\alpha_t^{(0)}$	1.6±0.8	0.44±0.38	0.32±0.24	1.0±0.4	−0.05±0.26	0.28±0.42	0.59±0.38
12	$\beta^{(1)}$	−6.4±3.3	−4.0±3.0	−5.5±1.2	−0.6±2.9	5.3±2.4	−5.3±4.4	−5.6±3.0
13	$\beta^{(0)}$	−22±6	−13±2	−12±1	−17±2	−9±2	−12±3	−12±2

1-*D* is even much larger than that of 1-*C*, which further illustrates the apparent incompatibility of $SU(3)$ and phases SPD-1.

In fit 1-*F* the ABC and K_1-K_1 terms are introduced. The resulting changes in other parameters are mostly not very great. In fact, fits 1-*B* and 1-*F* are rather similar. The ABC coupling constant assumes a value such as to make the ABC term relatively small. This is shown in Sec. III, where some matrix elements are tabulated. The K_1-K_1 exchange term is not so small. If ABC is replaced by the σ meson, the σ coupling constant turns out to be of the same order of magnitude as that of ABC; viz., $gh/4\pi(\sigma)=-0.40\pm0.40$. Other parameters are within 5% of the values of fit 1-*F*, except for $gh/4\pi(K_1\text{-}K_1)$ which increases by 30%.

In fit 1-*G* the four Y^* terms are omitted. Again the fit is quite similar to 1-*B*. This cannot be interpreted to mean that the sum of the Y^* contributions is small. The Y_0^*(1520 MeV) term, in particular, is quite large (cf. Sec. III). It seems that moderate changes in the background parameters compensate easily for the absence of the Y^* terms. This gives us some confidence in our procedure of neglecting the Y_0^*(1815 MeV) state. Because of its greater mass, this state should be even more amenable to representation by the background terms.

B. Phase Shifts SPD-2

In the first trial with the Yang-type phase shifts SPD-2 a violation of the constraint $G_{KN\Sigma}^2\geqslant 0$ occurred. This is shown in fit 2-*A* of Table IV. Fit 2-*B* is the corresponding best constrained fit, with $G_{KN\Sigma}=0$. The Λ and Σ coupling constants of fit 2-*B* are consistent with the inequalities (1.9) suggested by SU(3). However, these constants are not at all well determined by the data; the error of the Λ constant is very large, and the χ^2 increases by only 6% when $G_{KN\Sigma}^2/4\pi$ is changed from −24 (Fit 2-*A*) to zero (Fit 2-*B*). This situation is apparently due to the strong correlations between the Λ and Σ terms and the background which are evident in Table V. It seems that no distinctive effects of the Λ

TABLE V. Matrix of error correlation coefficients for fit 2-*A* of Table IV.

	1	2	2	4	5	6	7	8	9	10	11	12	13
1	1	−0.23	−0.51	0.17	0.01	0.69	−0.56	−0.58	0.56	−0.52	0.56	0.66	−0.55
2		1	0.77	−0.22	−0.16	0.50	0.93	−0.44	−0.87	−0.44	−0.87	0.42	0.91
3			1	−0.02	−0.11	0.12	0.81	−0.13	−0.73	−0.06	−0.75	0.21	0.76
4				1	−0.73	−0.17	−0.35	0.42	0.52	−0.60	0.53	−0.01	−0.38
5					1	0.12	−0.03	−0.45	−0.16	−0.48	−0.14	0.18	0.04
6						1	0.19	−0.94	−0.19	−0.88	−0.19	0.94	0.19
7							1	−0.21	−0.98	−0.25	−0.98	0.12	0.99
8								1	0.28	0.97	0.28	−0.90	−0.24
9									1	0.34	0.99	−0.12	−0.98
10										1	0.34	−0.77	−0.27
11											1	−0.11	−0.97
12												1	0.14
13													1

and Σ pole terms are visible in the data, just as in the earlier attempts at determining the Λ and Σ coupling constants mentioned in Sec. I.

Fit 2-*B* is also quite indifferent to the value of the χ (vector) coupling constant, judging from the large error ($\gamma_{\chi NN}{}^{(1)}\gamma_{\chi KK}/4\pi=4.8\pm3.4$). The result 4.8 ± 3.4 is consistent with the rough $SU(3)$ estimate of Eq. (1.15). The large error is partly due to the strong correlation with the other t-channel $I=0$ term, χ (tensor). The χ (vector) term also shows fairly large correlations with the α_s and α_t background terms.

The ρ coupling constant happens to be relatively well determined for phases SPD-2. The value $\gamma_{\rho NN}{}^{(1)}\gamma_{\rho KK}/4\pi=0.92\pm0.15$ of fit 2-*B* disagrees with the $SU(3)$ prediction Eq. (1.12) by two and one-half standard deviations. The discrepancy may have to do with the neglect of unitarity corrections. In Sec. IV a data fit is reported which is similar to fit 2-*B*, except for the inclusion of some sample unitarity integrals. The ρ coupling constant in that fit is $\gamma_{\rho NN}{}^{(1)}\gamma_{\rho KK}/4\pi=0.60\pm0.16$, in excellent agreement with Eq. (1.12). One should not be too satisfied with this result, however, since some doubts about the place of the ρ meson in the $SU(3)$ scheme have been raised by recent experiments. For example, preliminary results from the "missing mass spectrometer" at CERN show a resolution of the ρ peak into two peaks.[42] Possibly only one of these peaks can be associated with a vector octet, in which case Eq. (1.12) would not be correct.

To show that fit 2-*B* is not so very remote from the requirements of Eqs. (1.9) and (1.12) we present fit 2-*C*. Here the Λ and Σ coupling constants are given $SU(3)$ values corresponding to $f=0.35$, and the ρ constant the value of Eq. (1.12). The χ^2 rises from 55 to 64. The similar run for phases SPD-1 gave $\chi^2=141$.

It is interesting that the ρ exchange is quite essential in the fits to phases SPD-2. This is demonstrated by run 2-*D*, in which ρ is omitted. The χ^2 rises to the unacceptable and surprisingly large value of 94. Run 2-E shows that the χ exchange terms are also quite necessary. The χ^2 becomes 87 when both χ (vector) and χ (tensor) terms are omitted. In fit 2-*F* the ABC and K_1-K_1 exchanges are introduced, in addition to the terms of fit 2-*B*. The fits 2-*F* and 2-*B* are qualitatively similar, just as the corresponding fits 1-*B* and 1-*F* to phases SPD-1 were similar. It is curious that the ABC and K_1-K_1 coupling constants are nearly the same for phases SPD-2 as for SPD-1. For SPD-2 it is also noteworthy that the coupling constants for vector meson exchange are hardly affected by the introduction of ABC and K_1-K_1; the main differences between the fits 2-*B* and 2-*F* are in the Λ and background terms. Since the ABC exchange represents a force of long range, one might have thought that the long range vector meson terms would have been most perturbed by its introduction. In the last fit 2-*G* of Table IV the four Y^* terms are dropped. Again, the fit has a strong resemblance to fit 2-*B*, in the same way that the corresponding fits 1-*B* and 1-*G* resembled each other.

In acceptable fits to phases SPD-2 the background parameters do not show highly pronounced isospin dependence, in spite of the striking differences between $I=0$ and $I=1$ scattering. In fit 2-*B* the isospin dependences of $\alpha^{(I)}$, $\alpha_s{}^{(I)}$, and $\beta^{(I)}$ are consistent with that arising from an $I=1$ state in the u channel; viz., $(I=1)/(I=0)=\frac{1}{3}$. The $\alpha_t{}^{(I)}$ isospin behavior could be explained as the result of superposition of $I=1$ and $I=0$ states in the t channel.

In an attempt to assess the effects of combining the ω and φ contributions in the χ exchange term, we have performed a fit to phase shifts SPD-2 with separate φ and ω terms. This may not be very meaningful, since the coupling constants for the χ terms are already badly determined. The following fit is obtained, with $\chi^2=46$, $P(\chi^2)=0.44$:

$$G_{KN\Lambda}{}^2/4\pi=-3\pm17\,,\qquad G_{KN\Sigma}{}^2/4\pi=0\,,$$
$$\gamma_{\rho KK}\gamma_{\rho NN}{}^{(1)}/4\pi=0.72\pm0.16\,,$$
$$\gamma_{\omega KK}\gamma_{\omega NN}{}^{(1)}/4\pi=13\pm5\,,$$
$$\gamma_{\varphi KK}\gamma_{\varphi NN}{}^{(1)}/4\pi=-23\pm11\,,$$
$$\gamma_{\omega KK}\gamma_{\omega NN}{}^{(2)}/4\pi=9.6\pm3.8\,,$$
$$\gamma_{\varphi KK}\gamma_{\varphi NN}{}^{(2)}/4\pi=-23\pm8\,,$$
$$\alpha^{(1)}=-193\pm67\,,\qquad \alpha^{(0)}=-197\pm59\,,$$
$$\alpha_s{}^{(1)}=3.2\pm1.0\,,\qquad \alpha_s{}^{(0)}=3.3\pm0.9\,,$$
$$\alpha_t{}^{(1)}=2.2\pm0.6\,,\qquad \alpha_t{}^{(0)}=1.6\pm0.6\,,$$
$$\beta^{(1)}=-43\pm14\,,\qquad \beta^{(0)}=-47\pm12\,.$$

As usual, the constraint $G_{KN\Sigma}{}^2\geqslant0$ was imposed. Without constraint the Σ constant had the value $G_{KN\Sigma}{}^2/4\pi=-20\pm15$. The conclusions about the Λ, Σ, and ρ couplings in this fit are roughly the same as those of fit 2-*B*. On the other hand, the ω and φ terms together apparently do not approximate the χ term very well, since the background parameters have shifted considerably from their values of fit 2-*B*. We suspect, however, that is represents a statistical artifact resulting from too many parameters associated with $I=0$ vector mesons. One indication that separate ω and φ terms should not be included is that the correlation coefficients between the φ and ω terms are practically unity: $C_{\omega^{(1)}-\varphi^{(1)}}=-0.90$, $C_{\omega^{(2)}-\varphi^{(2)}}=-0.99$. Also, the values of the separate φ and ω coupling constants seem unreasonably large. There is a sort of dipole effect; the φ and ω terms are separately enormous, but their opposite signs result in a close cancellation. The background parameters in this fit have the curious property of being almost independent of isospin. In a similar fit to phases SPD-1, the φ-ω dipole effect does not occur. The inclusion of separate φ and ω terms is even less justified for phase shifts SPD-1, since we have shown that even the χ term is superfluous in fitting those phase shifts.

[42] B. Maglič, Invited Paper at the Argonne National Laboratory Symposium on Symmetries in Particle Dynamics, October 1964, Chicago, Illinois (unpublished).

III. BEHAVIOR OF SEPARATE TERMS OF THE SCATTERING AMPLITUDE

In this section we describe the separate constituents of the scattering amplitudes. Tables VI, VII, and VIII show the various single-particle exchange terms and background terms as functions of energy. Formulas for the functions tabulated are given in the Appendix. Coupling constants and isospin factors are omitted in the tables. To specify isospin factors, we denote by [Λ] and [Σ] any terms representing $I=0$ and $I=1$ states in the u channel, respectively. Similarly, [φ] and [ρ] denote contributions from $I=0$ and $I=1$ states of the t channel. The K-N scattering amplitudes are as follows:

$$\begin{aligned} f(I=1)&=[\Lambda]+[\Sigma]+[\varphi]+[\rho],\\ f(I=0)&=-[\Lambda]+3[\Sigma]+[\varphi]-3[\rho]. \end{aligned} \tag{3.1}$$

From Tables VI through VIII, Eq. (3.1), and the coupling constants given in Sec. I and Tables II and IV, the interested reader may evaluate approximately the various contributions to the amplitudes. The exact graphs plotted in Sec. II cannot be reproduced with the information tabulated, however; many more significant figures than we have stated would be necessary.

The graphs of Fig. 4(a)–(j) show an analysis of the amplitudes into constituents for the case of Yang-type phase shifts SPD-2. The amplitudes are from fit 2-B of Sec II, Table IV. In each graph the dashed curve represents $\sin\delta\cos\delta$, and is equal to the sum of the solid curves. Thus, the dashed curves are the same as the curves of Fig. 3, but plotted on a different scale. When the dashed curve does not appear, $\sin\delta\cos\delta$ is simply too small to show up on the same scale with its constituent terms. Note that the scale varies from one graph to the next in Fig. 4. The curve labeled Y^* represents the sum of the four Y^* contributions. As one can see from the tables, this sum is dominated by the Y_1^*(1385 MeV) and Y_0^*(1520 MeV) terms, with the latter term usually the larger. The curve labeled B represents the sum of the background terms. All four background terms contribute to states with $J=\frac{1}{2}$, while only the α_t term appears in $J=\frac{3}{2}$ states. The background terms do not contribute at all to $J=\frac{5}{2}$. This fact illustrates the short-range character of the background forces. The curve

TABLE VI. Partial-wave amplitudes for exchange of u-channel particles. Powers of ten are suppressed, except at column heads.

$P_{\rm lab}$ (MeV/c)	Λ	Σ	Y_0^*(1405)	Y_1^*(1385)	Y_0^*(1520)	Y_1^*(1660)
$s_{1/2}$						
235	−0.06201	−0.05920	0.09595	0.06381	−0.1290	−0.1788
385	−0.09597	−0.09186	0.1387	0.09437	−0.01533	−0.2122
505	−0.1189	−0.1141	0.1611	0.1119	0.2178	−0.1798
611	−0.1367	−0.1314	0.1742	0.1232	0.5313	−0.1077
710	−0.1513	−0.1457	0.1820	0.1307	0.9068	−0.006534
805	−0.1638	−0.1579	0.1863	0.1358	1.335	0.1184
$p_{1/2}$						
235	-0.3198×10^{-3}	-0.3329×10^{-3}	-0.2379×10^{-2}	0.1279×10^{-2}	-0.2623×10^{-1}	-0.0967×10^{-1}
385	−1.444	−1.234	−0.8647	0.5039	−1.015	−0.3759
505	−2.733	−2.348	−1.615	1.015	−2.010	−0.7469
611	−4.139	−3.574	−2.416	1.628	−3.168	−1.182
710	−5.598	−4.855	−3.229	2.325	−4.450	−1.666
805	−7.082	−6.167	−4.037	3.096	−5.824	−2.188
$p_{3/2}$						
235	0.08484×10^{-2}	0.06965×10^{-2}	-0.07894×10^{-2}	0.2956×10^{-3}	-0.2494×10^{-1}	-0.08259×10^{-1}
385	0.3086	0.2564	−0.2754	1.109	−1.013	−0.3358
505	0.5778	0.4848	−0.4948	2.116	−2.099	−0.6963
611	0.8669	0.7337	−0.7129	3.267	−3.456	−1.148
710	1.163	0.9916	−0.9191	4.462	−5.051	−1.679
805	1.460	1.253	−1.110	5.690	−6.872	−2.288
$d_{3/2}$						
235	0.03039×10^{-4}	0.02278×10^{-4}	0.02087×10^{-3}	0.02530×10^{-3}	-0.005175×10^{-2}	-0.01394×10^{-3}
385	0.2656	0.2012	0.1826	0.2378	−0.05114	−0.1389
505	0.7653	0.5853	0.5264	0.7320	−0.1649	−0.4513
611	1.521	1.174	1.046	1.547	−0.3634	−1.003
710	2.505	1.949	1.720	2.697	−0.6593	−1.830
805	3.693	2.894	2.531	4.191	−1.063	−2.970
$d_{5/2}$						
235	-0.01393×10^{-3}	-0.009832×10^{-3}	0.07793×10^{-4}	0.03008×10^{-4}	0.02090×10^{-2}	0.005709×10^{-2}
385	−0.1191	−0.08586	0.6563	0.2722	0.2050	0.05674
505	−0.3370	−0.2473	1.824	0.8085	0.6605	0.1840
611	−0.6598	−0.4917	3.498	1.649	1.455	0.4077
710	−1.073	−0.8099	5.565	2.778	2.636	0.7426
805	−1.563	−1.194	7.927	4.178	4.246	1.203

TABLE VII. Partial-wave amplitudes for exchange of t-channel particles. Powers of ten are suppressed, except at column heads.

$P_{\rm lab}$ (MeV/c)	ρ	$\chi^{(1)}$	$\omega^{(1)}$	$\varphi^{(1)}$	$\chi^{(2)}$	$\omega^{(2)}$	$\varphi^{(2)}$	ABC	σ	K_1-K_1
$s_{1/2}$										
235	-1.598×10^{-1}	-1.176×10^{-1}	-1.565×10^{-1}	-0.9421×10^{-1}	0.1450×10^{-2}	0.1919×10^{-2}	0.1166×10^{-2}	6.665×10^{-1}	4.683×10^{-1}	0.8690×10^{-1}
385	−2.269	−1.860	−2.426	−1.509	0.5467	0.7038	0.4473	7.490	5.640	1.266
505	−2.597	−2.351	−3.019	−1.928	1.058	1.332	0.8780	7.445	5.815	1.484
611	−2.770	−2.754	−3.492	−2.278	1.635	2.023	1.374	7.225	5.770	1.622
710	−2.851	−3.102	−3.893	−2.584	2.254	2.747	1.913	6.960	5.655	1.713
805	−2.872	−3.412	−4.243	−2.861	2.903	3.494	2.487	6.695	5.510	1.774
$p_{1/2}$										
235	-0.2945×10^{-1}	-0.5420×10^{-2}	-0.08114×10^{-1}	-0.4019×10^{-2}	-0.3223×10^{-2}	-0.4276×10^{-2}	-0.2586×10^{-2}	0.6895×10^{-1}	0.3330×10^{-1}	0.7020×10^{-3}
385	−1.043	−1.984	−0.2882	−1.496	−1.183	−1.532	−0.9647	1.368	0.7615	2.341
505	−1.915	−3.733	−0.5299	−2.855	−2.234	−2.836	−1.845	1.701	1.020	4.041
611	−2.829	−5.625	−0.7833	−4.356	−3.379	−4.217	−2.822	1.871	1.177	5.610
710	−3.747	−7.577	−1.038	−5.927	−4.566	−5.620	−3.849	1.956	1.272	6.985
805	−4.658	−9.550	−1.290	−7.540	−5.773	−7.019	−4.909	1.993	1.327	8.175
$p_{3/2}$										
235	0.1690×10^{-2}	-0.2034×10^{-2}	-0.3606×10^{-2}	-0.1306×10^{-2}	0.09167×10^{-2}	0.1231×10^{-2}	0.07309×10^{-2}	0.7315×10^{-1}	0.3625×10^{-1}	0.1252×10^{-2}
385	0.7062	−0.7540	−1.282	−0.4968	0.3453	0.4576	0.2773	1.480	0.8480	0.4322
505	1.455	−1.437	−2.362	−0.9676	0.6670	0.8734	0.5395	1.872	1.158	0.7705
611	2.346	−2.190	−3.506	−1.502	1.029	1.333	0.8382	2.092	1.359	1.103
710	3.332	−2.982	−4.666	−2.077	1.417	1.818	1.161	2.217	1.492	1.417
805	4.390	−3.798	−5.831	−2.682	1.824	2.318	1.503	2.288	1.581	1.707
$d_{3/2}$										
235	-0.07594×10^{-2}	-0.01008×10^{-2}	-0.02034×10^{-2}	-0.05935×10^{-3}	-0.05822×10^{-3}	-0.1004×10^{-3}	-0.03834×10^{-3}	0.9170×10^{-2}	0.3139×10^{-2}	0.01372×10^{-3}
385	−0.6132	−0.08646	−0.1656	−0.5248	−0.5018	−0.8260	−0.3404	3.281	1.397	0.1094
505	−1.658	−0.2452	−0.4503	−1.528	−1.430	−2.267	−0.9934	5.200	2.488	0.2896
611	−3.129	−0.4809	−0.8532	−3.063	−2.817	−4.326	−1.997	6.600	3.403	0.5320
710	−4.930	−0.7825	−1.349	−5.081	−4.604	−6.888	−3.323	7.605	4.134	0.8130
805	−6.999	−1.141	−1.918	−7.536	−6.739	−9.862	−4.943	8.330	4.710	1.117
$d_{5/2}$										
235	0.05035×10^{-3}	-0.04222×10^{-3}	-0.09965×10^{-3}	-0.02173×10^{-3}	0.01903×10^{-3}	0.03401×10^{-3}	0.01216×10^{-3}	0.9625×10^{-2}	0.3365×10^{-2}	0.0366×10^{-3}
385	0.4771	−0.3667	−0.8118	−0.1963	0.1677	0.2894	0.1095	3.498	1.526	0.1770
505	1.440	−1.052	−2.215	−0.5822	0.4875	0.8163	0.3242	5.620	2.759	0.4796
611	2.950	−2.086	−4.214	−1.187	0.9775	1.595	0.6608	7.220	3.824	0.9000
710	4.959	−3.432	−6.694	−2.000	1.623	2.589	1.114	8.410	4.703	1.406
805	7.418	−5.056	−9.580	−3.009	2.412	3.771	1.678	9.300	5.420	1.971

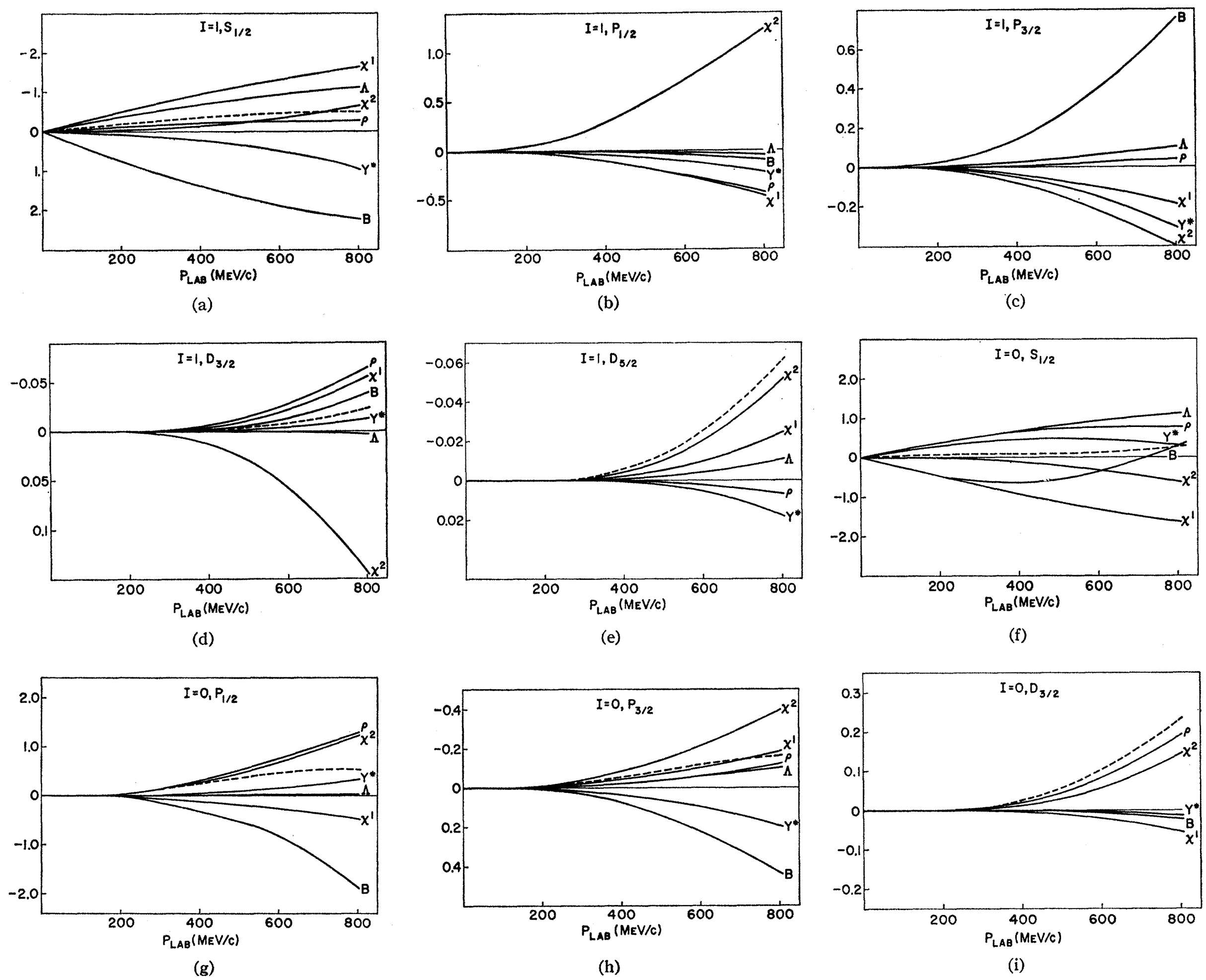

FIG. 4. Analysis of the amplitude for fit 2-B of Table IV. The dashed curve represents $\sin\delta\cos\delta$ for fit 2-B, and the sum of the solid curves is the dashed curve. The Y^* curve is the sum of the four Y^* contributions, while B indicates the sum of the background terms. When the dashed curve does not appear, $\sin\delta\cos\delta$ is too small to show up on the scale employed.

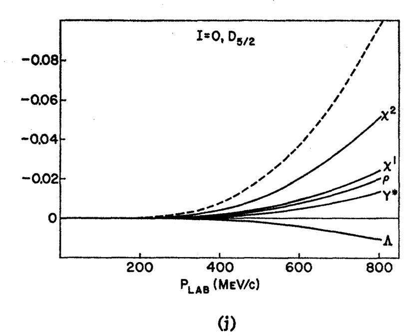

labeled ρ represents both the vector and the tensor terms, with a ratio given by Eq. (1.12). One can calculate approximately the separate vector and tensor contributions by referring to the $\omega^{(1)}$ and $\omega^{(2)}$ columns of Table VII, ignoring the small ρ-ω mass difference. The curves labeled χ^1 and χ^2 correspond to the vector and tensor contributions, respectively, of the fictitious particle χ which represents the average effect of φ and ω.

We now offer a few comments on outstanding features of the graphs of Figs. 4(a)–4(j). A noteworthy property of most of the amplitudes is the large magnitude of some of the separate terms. The physical amplitude is usually the result of a near cancellation between very large terms of opposite sign. Because of the large magnitude of the Y^* contributions it is clear that such cancellations *must* occur, and do not represent merely a fault of our theory. The Y^* coupling constants are essentially determined by experiment, so the Y^* graphs as shown must be taken seriously. The Y^* term is often much larger than the scattering amplitude itself.

In the $I=1$, $s_{1/2}$ state the Λ, ρ, and χ terms are all repulsive, as Fig. 4(a) indicates. Their sum amounts to

TABLE VIII. Partial-wave projections of the Cini-Fubini polynomials.

P_{lab} (MeV/c)	α	α_s	α_t	β
$s_{1/2}$				
235	0.05514	6.082	−0.1280	0.2086
385	0.08541	10.08	−0.5008	0.3538
505	0.1060	13.31	−1.003	0.4757
611	0.1220	16.27	−1.601	0.5890
710	0.1354	19.08	−2.276	0.6975
805	0.1468	21.82	−3.018	0.8034
$p_{1/2}$				
235	−0.0003492	−0.03851	0.04338	0.006013
385	−0.001337	−0.1577	0.1739	0.02350
505	−0.002620	−0.3291	0.3561	0.04696
611	−0.004095	−0.5458	0.5809	0.07479
710	−0.005702	−0.8035	0.8426	0.1060
805	−0.007410	−1.101	1.139	0.1401
$p_{3/2}$	α_t	$d_{3/2}$	α_t	
235	0.04257		−0.0002696	
385	0.1661		−0.002599	
505	0.3315		−0.008196	
611	0.5278		−0.01771	
710	0.7481		−0.03151	
805	0.9894		−0.04992	

a very big repulsive effect, which is partly canceled by the large, attractive Y^* term and an even larger background term. Since the Λ, ρ, and $\chi^{(1)}$ terms are more or less in accord with $SU(3)$ predictions, the $SU(3)$ scheme provides a partial explanation of the repulsive character of the $I=1$, $s_{1/2}$ state. (Admittedly, the repulsive character of the $\chi^{(1)}$ state is not a clear prediction of $SU(3)$; it will follow if the remarks preceding Eq. (1.15) serve to justify that equation.) In passing over to the $I=0$, $s_{1/2}$ state plotted in Fig. 4(b), the Λ and ρ terms are multiplied by -1 and -3, respectively, according to Eq. (3.1). The Y^* term remains attractive, because the isospin factor of 3 causes Y_1^*(1385 MeV) to dominate Y_0^*(1520 MeV). The peculiar energy dependence of the Y_0^*(1520 MeV) term evident in Table VI results in a pronounced downward turn of the total Y^* curve at the higher momenta. The larger ρ term levels off at the higher momenta, because of its component from the tensor rho-nucleon coupling. The experimental amplitude shows the opposite tendency from the ρ and Y^* terms; it curves upward at high momenta. The background term is able to compensate for ρ and Y^* and to produce the necessary rise. The background term has a surprisingly strong variation with energy. This behavior is possible because of close cancellations between the four large terms that make up the B curve. For example, at 805 MeV/c the separate $I=0$ background terms are as follows: $B(\alpha)=-11.6187$, $B(\alpha_s)=23.5130$, $B(\alpha_t)=-1.32400$, $B(\beta)=-10.2603$. Their sum is $B=0.3100$. Although the background terms represent short-range forces, in the sense that they do not contribute to angular momentum states with $J>\frac{3}{2}$, their sum may nevertheless show a highly nonlinear energy dependence in the s waves. These terms contain some high powers of momentum, which can become prominent in the sum if the low powers of momentum cancel each other. As we remarked in Sec. II, the background strength parameters have reasonable isospin dependence. This means that there are fairly close cancellations between four large terms in $I=1$ also. At 805 MeV/c in $I=1$ we have $B(\alpha)=-3.81242$, $B(\alpha_s)=11.6434$, $B(\alpha_t)=-2.31931$, $B(\beta)=-3.23530$, $B=2.2764$. A comparison of the $I=1$ and $I=0$ states shows that the ρ exchange has an important role in determining the isospin dependence of the $s_{1/2}$ scattering. The possibility of such an effect was pointed out by Sakurai[34] in connection with his gauge theory of vector mesons. In fact, Sakurai's suggestion was one of the motivations for our work. However, it turns out that the Λ and background terms are just as important as the ρ exchange in determining the isospin dependence. Thus the analogy with s-wave π-N scattering that Sakurai attempted to make is not quite complete. In the π-N problem the ρ exchange seems to be more prominent.

In the $I=1$, $p_{1/2}$ state of Fig. 4(c) we have the interesting situation of a strongly attractive $\chi^{(2)}$ exchange cancelling all of the other terms, which are repulsive. The cancellation is so perfect that the scattering amplitude is too small to plot on the same graph. Here the B term is much less prominent than in the other s- and p-wave states. In the $I=0$, $p_{1/2}$ state of Fig. 4(d) the $\chi^{(2)}$ term is, of course, the same as in $I=1$. It is joined by the ρ term, which is equally strong and attractive. Because of the dominance of Y_0^*(1520 MeV) in $p_{1/2}$, the Y^* contribution is also attractive. These three attractive terms are partly cancelled by $\chi^{(1)}$ and a substantial background term. Again we see that $SU(3)$ provides a partial explanation of the situation. It implies an attractive ρ exchange term of roughly the magnitude shown in Fig. 4(d); i.e., more than enough attraction to explain the data. As in $s_{1/2}$, the ρ term is important in explaining the isospin dependence of the scattering, but it is not dominant in this respect.

In the $I=1$, $p_{3/2}$ state [Fig. 4(e)] we once again have a nearly perfect cancellation between large terms, as in $I=1$, $p_{1/2}$. The situation is rather different, however, since the B term is much bigger in $p_{3/2}$. In the $I=0$, $p_{3/2}$ state the data are poor, but they vaguely suggest an attractive interaction. The Λ, ρ, $\chi^{(1)}$, and $\chi^{(2)}$ terms all give repulsive contributions in $I=0$ [Fig. 4(f)]; the theoretical amplitude is also repulsive. Improvement of the data in this state would be quite helpful for future work along these lines.

In the d waves, the ρ, $\chi^{(1)}$, and $\chi^{(2)}$ terms are generally the largest. In contrast to most of the lower angular momentum states, the background terms do not play a major role. Of course, this situation is in accord with the long-range character of the vector-meson exchange forces, and the short-range character of background forces. Improved data on the $I=0$ d waves would naturally be valuable in studying the long range forces. It seems quite reasonable in principle to allow d waves in the phase shift analyses above 400 or 500 MeV/c, since some of the separate single-particle exchanges produce substantial d-waves at those momenta. For example, the ρ term in our $I=0$, $d_{3/2}$ amplitude is non-negligible in magnitude, and it is also a term which must be taken seriously, since it has a magnitude roughly as prescribed by $SU(3)$.

An important characteristic of the graphs of Fig. 4 is the large magnitude of the $\chi^{(1)}$ and $\chi^{(2)}$ terms. Unfortunately, present theory does not make it possible to say whether such large effects from φ and ω exchange are reasonable or not. It may be that the best way to learn about φ and ω exchanges is to take information on the φNN and ωNN couplings from analysis of other experiments—for example, N-N scattering or nucleon electromagnetic structure experiments.

In the data fits tabulated in Sec. II the u-channel contribution of low-energy $\bar{K}$-N scattering has been omitted. For $\bar{K}$-N scattering between threshold and 400 MeV/c this omission is well justified. Table IX shows an evaluation of the relevant dispersion integrals based on the Humphrey-Ross[17] description of $\bar{K}$-N scattering. Expressions for the integrals evaluated are to be found in the Appendix. Table IX indicates that p- and d-wave integrals are entirely negligible, for either set of scattering lengths. The s-wave integrals are also practically negligible; they are smaller than the uncertainties arising from experimental errors and unitarity corrections (cf. Sec. IV).

TABLE IX. Integrals representing the effect of s-wave $\bar{K}$-N scattering. Solutions 1 and 2 are the two Humphrey-Ross $\bar{K}$-N scattering length solutions. The I values of the table refer to the *u channel*. Powers of ten are suppressed, except at column heads.

P_{lab} (MeV/c)	$s_{1/2}$	$p_{1/2}$	$p_{3/2}$	$d_{3/2}$	$d_{5/2}$
Solution No. 1, $I=1$					
235	0.57×10^{-2}	-0.13×10^{-3}	-0.42×10^{-4}	0.11×10^{-5}	0.37×10^{-6}
520	0.47	−0.48	−1.4	1.5	4.8
810	0.38	−0.79	−2.0	4.6	14
Solution No. 1, $I=0$					
235	1.8	−0.42	−1.3	0.33	1.2
520	1.5	−1.5	−4.3	4.6	15
810	1.2	−2.5	−6.5	14	43
Solution No. 2, $I=1$					
235	1.2	−0.29	−0.91	0.23	0.81
520	1.0	−1.0	−1.0	3.2	10
810	0.82	−1.7	−4.5	9.9	30
Solution No. 2, $I=0$					
235	1.1	−0.27	−0.86	0.21	0.76
520	0.96	−0.97	−2.8	3.0	9.9
810	0.77	−1.6	−4.2	9.3	28

IV. CORRECTIONS FOR UNITARITY

We assume a partial-wave dispersion relation for K-N scattering of the following form:

$$f(z)=g(z)+\frac{1}{\pi}\int_{w_0}^{\infty}\frac{\operatorname{Im}f(w+i0)dw}{w-z}. \qquad (4.1)$$

Here $z=s^{1/2}$ is the center-of-mass energy, and $w_0=m+\mu$ is the threshold energy of K-N scattering. The partial-wave amplitude $f(z)$ is defined so that $f(w+i0)=[\exp(2i\delta)-1]/2iq(w)$, $w>w_0$, where δ is the phase shift for a particular choice of angular momentum, parity, and isospin. The center-of-mass momentum is denoted by $q(w)$. The term $g(z)$ of Eq. (4.1) includes integrals over unphysical cuts, as well as an integral over a left-hand physical cut from $-\infty$ to $-w_0$. In our theory, g is represented by a sum of partial-wave projections of single-particle exchange terms, and partial-wave projections of the background terms of Eq. (1.2). Of course, this representation is expected to hold only in a low-energy physical interval $w_0\leqslant w<w_c$ and its immediate neighborhood. We are concerned with the real part of the integral over the right-hand physical cut. If this real part can be represented accurately by the background terms over the range of energy of our work, then the unitarity integral can be simply forgotten, and the theory is nevertheless effectively unitary.

We attempt to calculate the second term of Eq. (4.1) from experimental data. For orbital angular momentum $l\geqslant1$ we have the difficulty of meeting the threshold condition that $\operatorname{Re}f$ should behave as q^{2l} near $w=w_0$. In our approximation the function $g(w)$ satisfies the threshold condition. It follows that the second term of (4.1) must also satisfy it. Of course, the evaluation of this integral from experimental data is not likely to meet the threshold condition even approximately. Even in a complete theory, in fact, the integral is not expected to vanish at threshold.[43] Instead the term $g(w)$ is nonzero at threshold, cancelling against the integral. To remedy the situation in our incomplete theory, we write a dispersion relation for the quantity

$$h(z)=[(z-a)/(z-w_0)]^l f(z), \qquad (4.2)$$

where $a<w_0$ is a real constant. In this way Eq. (5.1) is replaced by

$$f(z)=\hat{g}(z)+\frac{1}{\pi}\left(\frac{z-w_0}{z-a}\right)^l \times\int_{w_0}^{\infty}dw'\left(\frac{w-a}{w'-w_0}\right)^l\frac{\operatorname{Im}f(w')}{w'-z}. \qquad (4.3)$$

The second term of (4.3) now has a threshold behavior like q^{2l} at $w=w_0$, but it also has a pole, in general, at $w=a$. In a complete theory this pole would be cancelled by a pole of opposite residue in $\hat{g}$. In fact, we have $\hat{g}(z)-g(z)=b/(z-a)^l$, while the difference between the integrals of (4.3) and (4.1) is $-b/(z-a)^l$. In order to get the right threshold behavior of f, we drop the pole term in $\hat{g}$; i.e., we take $\hat{g}=g$. Thus, the price of correct momentum dependence at threshold is the introduction of a new singularity at $z=a$. This singularity should not

[43] G. Frye and R. L. Warnock, Phys. Rev. 130, 478 (1963).

be too close to the physical threshold, since the single-particle exchanges are supposed to account for nearby singularities. We choose $a=0$, since the background terms already have poles at $w=0$. In fact, the w-plane singularities of the background terms are poles of orders one through four at $w=0$, and poles of orders one and two at infinity. Ideally, the background constants will adjust themselves so as to compensate properly for the pole of the unitarity integral. The singularity to be desired at $w=0$ in a complete theory is unknown, even if the Mandelstam representation is postulated. The question depends on the asymptotic behavior of double spectral functions.[43]

In evaluating the real part of the second term of Eq. (4.3), the following method proved useful in handling the principal value integration. Define φ by $\text{Im}f(w)=(w-w_0)^{1/2}\varphi(w)$, and subtract and add a term so that the principal value integral becomes

$$\frac{1}{\pi}\int_{w_0}^{\infty} dw'(w'-w_0)\left[\frac{\left(\frac{w'}{w'-w_0}\right)^l\varphi(w')-\frac{w}{w'}\left(\frac{w}{w-w_0}\right)^l\varphi(w)}{w'-w}\right] +w\varphi(w)\left(\frac{w}{w-w_0}\right)^l P\int_{w_0}^{\infty}\frac{dw'(w'-w_0)^{1/2}}{w'(w'-w)}. \quad (4.4)$$

Since the integral in the last term may be evaluated analytically, we avoid numerical evaluation of a principal value integral. After mapping the region of integration onto the interval [0,1] by the transformation $w=w_0/u^2$, we find

$$\frac{2}{\pi w_0^{\frac{1}{2}}}\int_0^1 du\, w'(w'-w_0)^{1/2} \times\left[\frac{w\left(\frac{w'}{w'-w_0}\right)^l\varphi(w')-w\left(\frac{w}{w-w_0}\right)^l\varphi(w)}{w'-w}\right] +w_0^{1/2}\left(\frac{w}{w-w_0}\right)^l\varphi(w). \quad (4.5)$$

The reason for factoring out $(w-w_0)^{1/2}$ is to keep the integrand finite; otherwise, the square bracket would be infinite at $w=w'=0$ in the $l=0$ case. The integral of Eq. (4.5) was evaluated by Simpson's rule with 100 intervals. Thus, nine points at which the integrand is evaluated lie in the experimental region 0–810 MeV/c. At these points the integrand is given values corresponding to the curves of Figs. 2 or 3. At the remaining 92 points outside the experimental region we must make some hypothesis about the behavior of the integrand. Above some energy it is common to assume that any particular partial wave is "completely absorbed"; i.e., that $\text{Im}f=1/2q$. We take this energy to correspond to $u=0.75$, where u is the integration variable of Eq. (4.5). The laboratory momentum corresponding to $u=0.75$ is 2.82 BeV/c. In the region $0.75\leqslant u\leqslant 0.90$ we try various hypotheses about the behavior of Imf. Specifically, we take the six different curves for $q\,\text{Im}f=\sin^2\delta$ tabulated in Table X, and we use the same six curves for all scattering amplitudes considered. The curves of Table X are chosen more for their disparity than for possible resemblance to reality. Curves 5 and 6 involve resonances, although there is no reason to think that resonances exist in the states we deal with. The states for which we calculate the integrals are $I=1$, $s_{1/2}$ and $I=0$, $p_{3/2}$ (for phase shifts SPD-1) or $I=0$, $p_{1/2}$ (for phase shifts SPD-2). These states involve the largest phase shifts, so if the unitarity corrections are small for these states they should be negligible for the others. The values of the integrals for the six different high-energy behaviors are shown in Table XI. The last column of the table shows an estimate of the uncertainty in the unitarity integral due to uncertainty in the high-energy behavior of Imf. The estimate is very crude; it is merely one half the difference between the largest and the smallest of the six integrals. The uncertainties increase sharply at the higher momenta. Most of the integrals decrease rapidly between 640 and 810 MeV/c.

TABLE X. Randomly chosen high-energy curves for $\sin^2\delta=q\,\text{Im}f$.

u	1	2	3	4	5	6
0.90	0.45	0.40	0.40	0.50	0.40	0.50
0.89	0.40	0.30	0.20	0.40	0.50	0.70
0.88	0.35	0.20	0.00	0.30	0.60	1.0
0.87	0.30	0.10	0.20	0.20	0.80	0.70
0.86	0.25	0.05	0.40	0.20	1.0	0.60
0.85	0.20	0.10	0.50	0.10	0.90	0.40
0.84	0.25	0.20	0.40	0.10	0.80	0.30
0.83	0.30	0.30	0.30	0.20	0.60	0.50
0.82	0.35	0.20	0.20	0.40	0.50	0.30
0.81	0.40	0.10	0.30	0.50	0.40	0.50
0.80	0.45	0.05	0.40	0.50	0.40	0.30
0.79	0.50	0.10	0.50	0.50	0.30	0.20
0.78	0.45	0.20	0.45	0.50	0.30	0.10
0.77	0.40	0.30	0.40	0.50	0.40	0.10
0.76	0.40	0.40	0.45	0.50	0.50	0.20
0.75	0.45	0.50	0.45	0.50	0.50	0.40

We have performed two fits to the data including the integrals of column 1 of Table XI. The fits are like fits 1-B and 2-B of Sec. II, except for the addition of the integrals and an increase of the experimental errors by amounts corresponding to the uncertainties listed in Table XI. The parameters of the two fits, labeled 1-BU and 2-BU, are shown in Table XII. The parameters are fairly close to the parameters of fits 1-B and 2-B. We take this as justification for the omission of unitarity integrals in the exploratory work of Sec. II. The χ^2 values for the fits with unitarity integrals are $\chi^2=35$, $P(\chi^2)=0.85$(1-BU) and $\chi^2=47$, $P(\chi^2)=0.41$(2-BU). Without unitarity integrals (consequently, with smaller

TABLE XI. Values of unitarity integrals. Powers of ten are suppressed, except at column heads.

P_{lab} (MeV/c)	1	2	3	4	5	6	σ
$I=1$, $S_{1/2}$							
235	3.05×10^{-2}	2.75×10^{-2}	2.98×10^{-2}	3.02×10^{-2}	3.49×10^{-2}	3.34×10^{-2}	0.004
355	4.32	3.83	4.20	4.27	5.02	4.80	0.006
520	5.02	4.21	4.78	4.93	6.18	5.86	0.010
640	4.62	3.48	4.24	4.50	6.25	5.89	0.014
810	1.95	0.05	1.10	1.77	4.61	4.41	0.023
$I=0$, $P_{3/2}$ (SPD-1)							
235	0.233×10^{-2}	0.211×10^{-2}	0.224×10^{-2}	0.229×10^{-2}	0.272×10^{-2}	0.265×10^{-2}	0.0003
355	0.622	0.549	0.589	0.611	0.752	0.731	0.001
520	1.54	1.32	1.44	1.51	1.94	1.89	0.006
640	2.08	1.66	1.85	2.02	2.84	2.78	0.012
810	0.648	−0.345	−0.035	0.539	2.30	2.44	0.014
$I=0$, $P_{1/2}$ (SPD-2)							
235	0.393×10^{-2}	0.371×10^{-2}	0.383×10^{-2}	0.389×10^{-2}	0.432×10^{-2}	0.425×10^{-2}	0.0003
355	0.925	0.851	0.892	0.913	1.05	1.03	0.001
520	2.14	1.92	2.04	2.11	2.54	2.49	0.003
640	0.991	0.565	0.760	0.927	1.74	1.69	0.006
810	−5.10	−6.09	−5.78	−5.21	−3.45	−3.30	0.014

TABLE XII. Parameter values for two fits to the data including the unitarity integrals of the first column of Table XI. Except for the unitarity integrals the fits 1-BU and 2-BU are like the fits 1-B and 2-B, respectively, of Tables II and IV.

	1-BU	2-BU		1-BU	2-BU
$G_{KN\Lambda}^2/4\pi$	0^+	1.6±16	$\alpha^{(1)}$	75±21	−43±38
$G_{KN\Sigma}^2/4\pi$	52±10	0^+	$\alpha^{(0)}$	269±55	−60±35
$\gamma_\rho NN^{(1)}\gamma_\rho KK/4\pi$	−0.53±0.21	0.60±0.16	$\alpha_s^{(1)}$	−0.39±0.24	0.70±0.36
$\gamma_\chi NN^{(1)}\gamma_\chi KK/4\pi$	2.9±3.3	5.7±3.5	$\alpha_s^{(0)}$	−1.8±0.4	0.86±0.32
$\gamma_\chi NN^{(2)}\gamma_\chi KK/4\pi$	−2.2±6.5	−22±6	$\alpha_t^{(1)}$	−0.17±0.25	0.91±0.36
			$\alpha_t^{(0)}$	−1.6±0.4	0.40±0.38
			$\beta^{(1)}$	5.7±2.6	−5.7±3.9
			$\beta^{(0)}$	25±5	−8.8±2.7

data errors) the corresponding values were $\chi^2=35$ and $\chi^2=55$.

Finally we note that the N/D method is a possible alternative to our method of handling unitarity corrections. However, the N/D calculation is considerably more difficult, and it has the serious disadvantage of developing ghost poles in s waves more often than not. Also, it cannot be directly applied to the Cini-Fubini representation, since the polynomial background terms have poles at infinity. The background terms would have to be approximated over the low-energy region by some functions with better asymptotic behavior.

V. COMPARISONS WITH EARLIER WORK AND CONCLUSIONS

Without pretensions of completeness, we mention some of the earlier work on K-N scattering. In 1957 and 1958, Yamaguchi[44] and Barshay[45] suggested that exchange of two pions in a nonresonant state might be an important effect. Although this effect is now thought to be of minor importance, the work of Yamaguchi and Barshay did call attention to possible interesting features of boson exchange. In 1959, Warnock[46] calculated K-N scattering by an N/D formula, taking the Λ and Σ Born terms for the N function. Pseudoscalar KNY coupling gave the best fit to the available K_+-p total cross sections, but the energy dependence of the data was fitted only by virtue of fairly strong $p_{3/2}$ scattering coming in at the higher energies. Later data suggest that p waves are almost absent below 810 MeV/c.

In 1960 and 1961, when the existence of the ρ meson was predicted but not yet confirmed, Lee[47] and Ferrari, Frye, and Pusterla[48] investigated the long-range part of the ρ contribution, taking $m_\rho\approx 500$ MeV. Lee was able to fit the available effective-range formulas for $I=1$

[44] Y. Yamaguchi, Proceedings of the Padua-Venice Conference, 1957 (unpublished); Progr. Theoret. Phys. Suppl. **11**, 37 (1959).
[45] S. Barshay, Phys. Rev. **110**, 743 (1958).
[46] R. L. Warnock, PhD dissertation, Harvard, 1959 (unpublished).
[47] B. W. Lee, PhD dissertation, University of Pennsylvania, 1960 (unpublished); Phys. Rev. **121**, 1550 (1961).
[48] F. Ferrari, G. Frye, and M. Pusterla, Phys. Rev. **123**, 315 (1961).

and $I=0$ scattering by a combination of a subtraction constant (or a distant pole) representing the short-range forces and a nearby pole representing the ρ. Both Lee and Ferrari *et al.* worked out much of the formalism of double-dispersion relations as it applies to K-N scattering. Lee suggested the application of the Cini-Fubini representation to the problem. Islam,[49] in 1961, allowed Λ and Σ as well as ρ, and was able to get rough, qualitative agreement with $I=1$ and $I=0$ data by adjusting the Λ and Σ coupling constants. He invoked a cancellation between the ρ and Λ, Σ terms to eliminate p waves in the $I=1$ state.

Between 1961 and 1964, a number of papers appeared in which various single-particle exchanges were included (e.g., ρ, ω, Λ, Σ, Y^*). A bibliography may be found in Ref. 50; see also Ref. 51. These studies are all incomplete in view of present knowledge; they omit some known particles which might be important, or they do not fit all recent scattering data, or they are unsatisfactory in principle because of the presence of nearby ghost poles in the scattering amplitude. In our opinion they also give insufficient attention to the part of the amplitude not represented by single-particle exchanges; i.e., the part we have called the background.

Recently Martin and Spearman[51] have carried out a more careful and thorough analysis of K_+-p scattering. They give particular attention to exchange of a light two-pion state—say ABC state. All other forces are represented by two poles in each partial-wave amplitude. One pole is very distant; it should have the same effect as our background terms. The other pole is at a location appropriate for representing a medium-range force. It is located at a point which would be the beginning of a branch cut due to a t-channel state of mass 880 MeV. There is also a singularity (not mentioned explicitly by Martin and Spearman) due to extraction of a "kinematical factor" [cf. their Eq. (4.2)]. In their notation, it is a branch point of the form $C(\nu+M^2)^{-1/2}$ in the scattering amplitude $f(\nu)$. The parameter M^2 is chosen so as to make this singularity fall near the beginning of the ρ and ω cuts. The constant C is not adjustable independently of the pole residues. In addition, there may be a ghost pole (i.e., a spurious zero of the D function) in the $I=1$, $s_{1/2}$ amplitude of Martin and Spearman. Apparently the question has not been investigated. Roy[51] and Costa, Zimerman, and Gluckstern[52] found ghost poles near the physical region in calculations quite similar to that of Martin and Spearman. It is not clear to us *a priori* that the combination of singularities used by Martin and Spearman represents adequately the effects of ρ and ω exchange. However, Martin and Spearman report in a private communication that their results are stable against large changes in M^2 and the pole positions. This may be construed as an argument in favor of their model. In any case, they are able to determine the strength of the singularity associated with the low-energy two-pion interaction. They find that this term is relatively small, in qualitative agreement with our conclusions.

Feshbach and Lomon[53] have applied their "boundary-condition model" to s-wave K_+-p scattering. Here the force of longest range is represented by a two-pion exchange potential, while all forces of shorter range are accounted for by placing an energy-independent boundary condition on the wave function at some interparticle distance r_0. *A priori* estimates of r_0 can be obtained by looking at Feynman graphs.[53] The arguments employed are closely related to those of Cini and Fubini.[2] It seems that the value of r_0 used in K_+-p scattering is consistent with an important role for ρ and ω exchanges.

To conclude, we comment on the prospects for future progress. From the work of Secs. II and III it seems that our picture of K-N scattering is acceptable if the correct $I=0$ phase shift set is the Yang-type set labeled SPD-2. On the other hand, the parameter values in the fits to Fermi-type phases SPD-1 are entirely out of line with theoretical predictions and with the earlier determination of the average of Λ and Σ coupling constants by forward-angle dispersion relations. Thus, a resolution of the Fermi-Yang ambiguity would provide a clear test of our theory. Such a test is interesting for its implications beyond the K-N problem, since one would like to build up a general confidence in the representation of the scattering amplitude as single-particle exchange terms plus background. Such a representation, which can be viewed as a generalized effective-range expansion, is expected to become more and more valuable as the quality of data improves.

Aside from the resolution of the Fermi-Yang ambiguity, the experimental progress that would help most would be improved accuracy for the $I=0$ phase shifts below 800 MeV/c. Data above 800 MeV/c in both $I=1$ and $I=0$ are potentially useful, but in this region one has the difficulties of multiple phase shift solutions, inelasticity, and the need for careful unitarity corrections. Whatever the difficulties, $I=1$ and $I=0$ phase shifts at the highest possible energies would be interesting, either as data points to be fitted or as an aid to estimating unitarity integrals.

In our fits with the Yang-type phase shifts SPD-2, we have some doubt about the treatment of the ω and φ exchanges. Since the average ω-φ term is quite prominent in the fits, it is essential to clarify the situation. It seems unlikely that the necessary ω and φ coupling constants can be determined from K-N scattering alone. It may be more feasible to take information on

[49] M. M. Islam, Nuovo Cimento **20**, 546 (1961).
[50] A. D. Martin and T. D. Spearman, Phys. Rev. **136**, B1480 (1964).
[51] D. P. Roy, Phys. Rev. **136**, B804 (1964).
[52] G. Costa, A. H. Zimerman, and R. L. Gluckstern, Proceedings of the Eastern Theoretical Physics Conference, 1962; Gordon and Breach, Science Publishers, Inc., New York, 1963.
[53] H. Feshbach and E. L. Lomon, Ann. Phys. (N. Y.) **29**, 19 (1964).

the ωNN and φNN coupling constants from N-N and e-N scattering. In a following paper we intend to try out that procedure.

ACKNOWLEDGMENTS

This project was conceived while both of us were fortunate to be at the Physics Department of the University of Washington. We want to thank Professor Boris Jacobsohn, Professor Ernest Henley, and the other people at Washington for their warm hospitality. During the later stages of the work one of us (R. Warnock) enjoyed a stay at the Physics Division of the Aspen Institute for Humanistic Studies, and a summer appointment in the High Energy Physics Division of Argonne National Laboratory. He wishes to thank Professor Robert Sachs for his hospitality at the latter institution.

The computations were carried out with the IBM 7090 computer at the Research Institute of Illinois Institute of Technology, and with the CDC 3600 at Argonne. Mary Wrenn and Dr. Howard Schmeising were very helpful with advice on programming.

Finally, we owe the greatest thanks to Dr. V. J. Stenger, who made his phase-shift analysis available before publication.

APPENDIX

For the reader's convenience we collect the formulas for partial-wave projections of single-particle exchange terms and background terms. The partial-wave amplitudes are related to partial-wave projections of the invariant amplitudes A and B by the following standard formula for $f=\sin\delta\, e^{i\delta}/q$[54]:

$$16\pi w f_{l\pm}(w)=(E+m)[A_l+(w-m)B_l] + (E+m)[-A_{l\pm1}+(w+m)B_{l\pm1}]. \quad \text{(A1)}$$

f_{l+} and f_{l-} are the two amplitudes for a given J; f_{l+} has $l=J-\frac{1}{2}$, while f_{l-} has $l=J+\frac{1}{2}$. The nucleon and K meson masses are denoted by m and μ, respectively, and w denotes the total energy in the center-of-mass frame. The nucleon energy E is given by the formula

$$E\pm m=[(w\pm m)^2-\mu^2]/2w. \quad \text{(A2)}$$

The total momentum in the center-of-mass frame is labeled q; thus, $q^2=(E+m)(E-m)$.

For exchange of a $J=\frac{1}{2}$ particle Y in the u channel, the projections of the invariant amplitudes are well-known[54]:

$$\begin{aligned} A_l&=-G^2(m+p_Y m_Y)Q_l(x)/q^2,\\ B_l&=G^2Q_l(x)/q^2,\\ x&=1+[\Sigma-s-m_Y^2]/2q^2,\\ \Sigma&=2(m^2+\mu^2);\quad s=w^2. \end{aligned} \quad \text{(A3)}$$

G is the coupling constant of Eq. (1.3a), and m_Y and p_Y are the mass and parity of the exchanged particle; $p_Y=-1$ for $Y=\Lambda$, Σ and $p_Y=1$ for $Y=Y_0^*$(1405 MeV). Q_l is the Legendre function of the second kind:

$$Q_l(x)=\frac{1}{2}\int_{-1}^{1}\frac{P_l(t)dt}{x-t}. \quad \text{(A4)}$$

Q_l may be expressed in terms of logarithms.[55]

In the case of a $J^P=\frac{3}{2}^+$ particle Y in the u channel, we begin with a fixed-t dispersion relation for K-N scattering[1]:

$$A(s,t)=\frac{1}{\pi}\int_{s_0}^{\infty}\frac{A_1(s',t)ds'}{s'-s}+\frac{1}{\pi}\int_{u_0}^{\infty}\frac{A_2(u',t)du'}{u'-u} + (\text{single spectral integrals}). \quad \text{(A5)}$$

A similar relation holds for $B(s,t)$. We retain only the term proportional to $\mathrm{Im} f_{1+}(u')$ in the partial-wave expansions[54] of $A_2(u',t)$ and $B_2(u',t)$, and set $\mathrm{Im} f_{1+}(u')=(\pi/2)\alpha\delta(u'^{1/2}-m_Y)$. After some calculation the following expressions are obtained:

$$\begin{aligned} A_l&=2b\delta_{l0}-[a+b(\Sigma-s-m_Y^2)]Q_l(x)/q^2,\\ B_l&=-2d\delta_{l0}+[c+d(\Sigma-s-m_Y^2)]Q_l(x)/q^2,\\ a&=4\pi\alpha m_Y\left[3\frac{m_Y+m}{E_Y+m}+\frac{m_Y-m}{E_Y-m}\right],\\ b&=4\pi\alpha m_Y\left[\frac{3}{2q_Y^2}\frac{m_Y+m}{E_Y+m}\right],\\ c&=4\pi\alpha m_Y\left[\frac{3}{E_Y+m}-\frac{1}{E_Y-m}\right],\\ d&=b/(m_Y+m). \end{aligned} \quad \text{(A6)}$$

Here Σ and x are defined as in Eq. (A3); E_Y and q_Y are the nucleon energy and the $\bar{K}$-N momentum at energy m_Y. The KNY coupling parameter α is related to the coupling constant H by Eq. (1.4). The amplitudes given in Table VI represent $f_{l\pm}$ divided by $H^2/4\pi$. Equation (A6) and Eq. (A1) yield the amplitude $f_{l\pm}{}^{3/2+}(w;m_Y)$ for exchange of a $\frac{3}{2}^+$ particle of mass m_Y. For $\frac{3}{2}^-$ exchange one may apply the identity

$$f_{l\pm}{}^{3/2-}(w;m_Y)=-f_{l\pm}{}^{3/2+}(w;-m_Y). \quad \text{(A7)}$$

For exchange of a 0^+ particle of mass μ_s in the t channel the formulas are

$$\begin{aligned} A_l&=mghQ_l(y)/q^2;\quad B_l=0,\\ y&=1+\mu_s^2/2q^2, \end{aligned} \quad \text{(A8)}$$

where g and h are the coupling parameters of Eq. (1.3c). For exchange of a 1^- particle with mass μ_v and vector coupling to the nucleon we have

$$\begin{aligned} A_l&=0;\quad B_l=-2\gamma\gamma^{(1)}Q_l(y)/q^2,\\ y&=1+\mu_v^2/2q^2, \end{aligned} \quad \text{(A9)}$$

with γ and $\gamma^{(1)}$ as defined in Eq. (1.3d). For 1^- exchange

[54] S. Frautschi and J. Walecka, Phys. Rev. **120**, 1486 (1960); W. Frazer and J. Fulco, *ibid.* **119**, 1420 (1960).

[55] E. Jahnke and F. Emde, *Tables of Functions with Formulas and Curves* (Dover Publications, Inc., New York, 1945).

with tensor coupling, both A_l and B_l are nonzero:

$$A_l = -(\gamma\gamma^{(2)}/m)[(\Sigma/2-\mu_v^2/2-s)Q_l(y)/q^2+\delta_{l0}],$$
$$B_l = -2\gamma\gamma^{(2)}Q_l(y)/q^2, \tag{A10}$$

where Σ and y are defined in Eq. (A3) and Eq. (A9), and γ, $\gamma^{(2)}$ in Eq. (1.3d). We found that in one version of FORTRAN the logarithm subroutine was not accurate enough for evaluation of the Q_l's in vector-meson exchange at low energies. The asymptotic expansion of $Q_l(x)$ for large x solved the problem.[55]

To indicate the partial-wave projections of the background terms of Eq. (1.1), we write out the partial-wave amplitudes in full.

$$\begin{aligned}
8\pi w f_{0+} &= (E+m)[\alpha+(w-m)\beta+s\alpha_s] \\
&\quad -2q^2[E+m+(E-m)/3]\alpha_t, \\
8\pi w f_{1-} &= -(E-m)[\alpha-(w+m)\beta+s\alpha_s] \\
&\quad +2q^2[E-m+(E+m)/3]\alpha_t, \\
12\pi w f_{1+} &= q^2(E+m)\alpha_t, \\
12\pi w f_{2-} &= -q^2(E-m)\alpha_t.
\end{aligned} \tag{A11}$$

The contribution of s-wave $\bar{K}$-N scattering in the u-channel is given by the following integrals:

$$A_l = \frac{-4}{q^2}\int_{s_0}^{s_m} ds' \frac{w'+m}{E'+m} Q_l(x')\,\mathrm{Im}f_{0+}(s'),$$
$$B_l = \frac{4}{q^2}\int_{s_0}^{s_m} ds' \frac{1}{E'+m} Q_l(x')\,\mathrm{Im}f_{0+}(s'), \tag{A12}$$
$$x' = 1+(\Sigma-s'-s)/2q^2;\quad s_0 = m+\mu.$$

In our calculations, the upper limit s_m corresponded to 400 MeV/c laboratory momentum, and the $\bar{K}$-N scattering amplitude was calculated in the complex-scattering-length approximation $q\cot\delta = 1/(a+ib)$. Thus,

$$\mathrm{Im}f_{0+}(s) = \frac{b+q(a^2+b^2)}{(1+qb)^2+q^2a^2}. \tag{A13}$$